Université de Montréal

Analyzing KDM4A protein interaction network using proximity-dependent biotin identification assay

Par

Rana Rizk

Faculté de Médecine

Thèse (ou Mémoire) présenté(e) en vue de l'obtention du grade de Maitrise

en Sciences Biomédicales, option Médecine Expérimentale

Août 2020

Université de Montréal

Unité académique : Faculté de Médecine

Ce mémoire (ou cette thèse) intitulé(e)

Analyzing KDM4A protein interaction network using proximity-dependent biotin identification assay

Présenté par

Rana Rizk

A été évalué(e) par un jury composé des personnes suivantes

Gerardo Ferbeyre
Président-rapporteur

Frédérick Antoine Mallette
Directeur de recherche

Serge McGraw
Membre du jury

Résumé

Cette étude a été conçue pour identifier les protéines qui interagissent potentiellement avec Déméthylase 4A spécifique de la lysine (KDM4A) dans le contexte du cancer en utilisant l'essai d'identification de la biotine dépendante de la proximité 2 (BioID2). KDM4A est une lysine déméthylase et un régulateur épigénétique qui joue un rôle dans la carcinogenèse en favorisant la prolifération. Nous avons cherché à identifier l'interactome protéique de KDM4A dans la lignée cellulaire du cancer du col de l'utérus HeLa. Ces interactions protéiques ont été caractérisées en fonction de leur dépendance à l'activité catalytique de KDM4A et / ou au domaine Tandem Tudor. De nouveaux interactants de KDM4A ont été détectés, tout en observant des partenaires protéiques précédemment identifiés, comme FBXO22. KDM4A semble interagir avec certains membres du complexe de remodelage de la chromatine pBAF, en particulier, ARID2, BRD7 et SMARCA2. Le complexe pBAF facilite ou empêche l'accessibilité à l'ADN en restructurant le nucléosome. Une analyse plus approfondie est nécessaire pour valider si l'interaction complexe KDM4A-pBAF est directe ou indirecte. Cette étude suggère également l'importance du domaine Tandem Tudor dans le rôle de KDM4A dans la réparation de bris double brin. Enfin, nous proposons également une implication potentielle de KDM4A dans l'épissage de l'ARNm et le transport d'anions organiques. Cette étude fournit de nouvelles informations sur le rôle de KDM4A dans le développement du cancer.

Mots-clés : KDM4A, JMJD2A, BioID2, cancer, pBAF, FBXO22, ARID2, ELAVL2, SLC16A3/1, SLC2A1.

Abstract

This study was designed to identify potential interacting proteins of Lysine-specific demethylase 4A (KDM4A) in the context of cancer using proximity-dependent biotin identification 2 (BioID2) assay. KDM4A is a lysine demethylase and an epigenetic regulator that plays a role in carcinogenesis by promoting proliferation. Herein, we sought out to identify the protein interactome of KDM4A in cervical cancer cell line HeLa. These protein interactions were characterized by their dependency on KDM4A's catalytic activity and/or Tandem Tudor domain. It succeeded at detecting novel interactors of KDM4A as well as previously studied interactions, such as FBXO22. KDM4A seems to be interacting with some members of the pBAF chromatin remodeling complex, specifically, ARID2, BRD7, and SMARCA2. The pBAF complex facilitates or prevents accessibility to DNA by restructuring the nucleosome. Further analysis is required to validate whether the KDM4A-pBAF complex interaction is direct or indirect. This study also implied the importance of the Tandem Tudor domain in KDM4A's role in the double stranded break repair. Finally, we also propose the potential involvement of KDM4A in mRNA splicing and organic anion transport. This study provides new insights into KDM4A's role in cancer development.

Keywords: KDM4A, JMJD2A, BioID2, cancer, pBAF, FBXO22, ARID2, ELAVL2, SLC16A3/1, SLC2A1.

Table des matières

Liste des tableaux

Liste des figures

Liste des sigles et abréviations

AU: adenylate/uridylate

AMP: ampicillin

AP1: activating protein 1

APEX: ascorbate peroxidase

BioID: proximity-dependent biotin identification

BRM: BRAHMA

BRCA1: breast cancer-associated gene 1

CDH5: chromodomain helicase DNA-binding domain 5

CDT1: chromatin licensing and DNA replication factor 1

CDK: Cyclin-dependent kinases

CDKIs: CDK inhibitors

CDC6: cell division control protein 6

ChIP: chromatin IP

COX-2: cyclooxygenase-2

DDR: DNA damage response

DEPTOR: DEP domain-containing mTOR-interacting protein

DOX: doxycycline

DSBs: double-strand breaks

ER: estrogen receptor

ETV1: ETS variant 1

E2F1: E2F transcription factor 1

Fe(II): iron

FXR1: fragile X-related protein 1

G: gap

GST: Glutamine S-transferase

H: histone

HDAC1: histone deacetylase 1

HER2: human epidermal growth factor receptor 2

HPV: human papillomavirus

HR: homologous repair

HRP: horseradish peroxidase

IF: immunofluorescence

IFIT1: interferon-induced transmembrane protein 1

IL-6: interleukin 6

IL-8: interleukin 8

IMR90: cultured human primary lung fibroblasts

IP: immunoprecipitation

JMJD2: jumonJi C domain-containing 2

K: lysine

KDM4: lysine demethylase 4

KAN: kanamycin

LH: luteinizing hormone

LE: luminal epithelium

M: metaphase

MCM: minichromosome maintenance complex

MDC1: mediator of the DNA damage checkpoint protein 1

miR: microRNA

MRN: MRE11/Rad50/NBS1

MS: mass spectrometry

mTOR: mammalian target of rapamycin

NCOR1: nuclear receptor co-repressor 1

NHEJ: non-homologous end-joining

NHS: *N*-hydroxysuxxinimide

NK: natural killer cells

NLS: nuclear localization signal

OIS: oncogene induced senescence

OPN: osteopontin

ORC: origin of replication complex

PDK1: phosphoinositide-dependent kinase-1

PHD: plant homeodomain

PI3K: phosphoInositide 3-kinase

pRB: retinoblastoma protein

PTEN: PI3,4,5-P_3

RI: restriction site

RNF: RING finger protein

S: synthesis

SASP: senescence-associated secretory phenotype

sat2: satellite 2 DNA

SSBs: single stranded breaks

TET: tetracycline

TT: tandem tudor

WB: western blot

WPRE*:* woodchuck hepatitis virus posttranscriptional regulatory element

w/: with

w/o: without

αKG: α-ketoglutarate

γH2AX: phosphorylation of the H2AX

53BP1: p53-binding protein 1

2HG: R-2-hydroxyglutarate

I would like to dedicate this thesis to my husband, my family and my friends who gave me all the love and the support I needed to complete my degree.

Remerciements

First and foremost, I would like to thank my supervisor Frederick, who has guided and helped me all throughout my degree. I also want to thank all the laboratory members, especially Karine Boulay, Dagmar Glatz, Erlinda Fernández Díaz, Christina Sawchyn, and Tabitha Rosembert, who have helped me when I needed it the most. Finally, I want to thank the Faculty of Medicine for providing me with a scholarship that spanned my degree.

Chapter 1 – Introduction

1.1 Cell proliferation and cancer

Cell proliferation is characterized by an increase in cell number and the degree of proliferation is measured as a function of time (1,76). Proliferation is a product of the mitotic cell cycle in which the cell undergoes division (1). There are two major phases in cell division and two time gaps that separate them. The two major phases are Synthesis (S) phase and Mitosis (M) phase (1,77). DNA is synthesized during the S-phase and the cell is divided during the M-phase (77). Gap 1 (G1) is the preparation phase for cells to enter the cell cycle, whereas Gap 2 (G2) is the preparation phase for cell division. Generally, G0 cells are non-dividing cells (1).

Normal cell growth is regulated by different growth factors and/or hormones. Cyclins are the main growth regulators of the cell cycle (2). They form complexes with cyclin-dependent kinases (CDK) to regulate the stages of the cell cycle (2,78). Cyclin-CDK complexes are differentially expressed during cell cycle progression and one way this expression can controlled is by CDK inhibitors (CDKIs). CDKIs are made up of two families, INK4 ($p16^{INK4a}$, $p15^{INK4b}$, $p18^{INK4c}$, $p19^{INK4d}$) and Cip/Kip ($p21^{cip1/waf1}$, $P27^{kip1}$, $p57^{kip2}$) inhibitors (2). Cyclin-CDK complexes and their antagonists CDKIs are direct regulators of cell cycle progression that control the cell's transition into the major stages of the cell cycle, the S-phase and M-phase, through checkpoints. The three major checkpoints are: G_1/S-phase transition checkpoint, G_2/M-phase transition checkpoint, and the spindle checkpoint in the M-phase (1,2,77). Failure to pass these checkpoints could result in apoptosis also known as controlled cell death (2).

Human cancers are characterized by uncontrolled cell proliferation that could be due in part for the loss of these cell cycle checkpoints (3,79). The dysregulation of the cell cycle components that make up these checkpoints is a result of altered genomic expression (3). Proteins such as pRB, p53, p21, and p16 play an important role in regulating the cell cycle in case of cellular stresses (3,14-19,79). Under conditions favoring proliferation, pRb (Retinoblastoma protein) is phosphorylated by cyclin-D-CDK4 and cyclin-D-CDK6 or cyclin-E-CDK2 complexes (3). Altering the activity of these complexes would result in pRB hypophosphorylation and cell cycle arrest

(3,19). Furthermore, progression through the cell cycle is dependent on adequate pRB phosphorylation. For instance, following subjection to genotoxic compounds, p53 tumor suppressor activates the transcription of p21 which inactivates cylin-E-CDK2 complexes, resulting in the hypophosphorylation of pRb and cell cycle arrest (3). Another pathway that results in cell cycle arrest is p16 activation, which is independent of p53. In this pathway, cyclin-D-CDK4 and cyclin-D-CDK6 are inactivated by p16, which leads to pRb hypophosphorylation and cell cycle arrest (3,14-18). Alteration in the gene expression of any of these components is found in most tumors and promotes continuous unregulated cell proliferation (3,81).

Moreover, cyclin-D loci are amplified in most human cancers (4,79). As mentioned earlier, cyclin D complexes with CDK4/6 (3). In current breast cancer research, targeting CDK4/6 is showing prominent results, where the disease progression was delayed in human epidermal growth factor receptor 2 (HER2) +, estrogen receptor (ER) + postmenopausal women (4). Cyclin E locus amplification is not as common but is still present in some human cancers (4,80). However, inhibitors targeting CDK2, the interacting partner of cyclin E, are not efficient and seem to present severe side-effects (4). Additionally, the gene loci of the INK4 CDKI proteins, which block primarily cyclin D-CDK4/6, are either mutated, deleted or epigenetically repressed (4). Mutated and deleted INK4 proteins cannot be reactivated, but the repression of INK4 gene loci with extensive CpG methylation can be reactivated since DNA methylation is reversible (4,82).

In addition, altered INK4 protein activities can be compensated through the administration of chemical CDKIs, such as flavopiridol, as cancer treatment (4,83). Flavopiridol can inhibit CDK2, CDK4 and CDK1 and seems to have an efficient anti-proliferative activity towards different types of cancers (4). However, patients who are subjected to this drug experience severe side-effects (3,4). These unwanted side-effects result from the feeble specificity of this drug to its intended targets (3). Additionally, current cancer treatments that target highly proliferative cells are also targeting normal cells that rapidly proliferate-- cells that are present in the skin, hair and gastrointestinal tract-- making these treatments very toxic (4,83). Consequently, a call for a more targeted approach is needed to diminish treatment toxicity and increase specificity and efficacy (4).

1.1.1 Epigenetic regulators

It was first assumed that mutations in the gene lead to differential gene expression (5,84,85). This assumption was quickly remodeled to include epigenetic events, which are the alteration in gene expression due to DNA methylation, histone modification, non-coding RNA activity, and chromatin remodeling (5,85). Notably, changes in gene expression due to epigenetic alterations occur by the addition or the removal of chemical groups from DNA and histones (5-9). These alterations are regulated by epigenetic regulators, which are divided into three groups: writers, erasers and readers. These groups consist of enzymes that carry out activities resembling their group name: “writers” add or transfer chemical groups on/to DNA or histones; “erasers” remove these chemical modifications from DNA or histones; “readers” recognize the alterations on DNA or histones (5). Subsequently, epigenetic regulators cooperate with other regulatory factors, such as transcription factors, to alter gene expression according to the modifications (5-7). Some examples of epigenetic regulators include: DNA methyltransferases, histone acetyltransferases, histone methyltransferases (writers); DNA-demethylating enzymes, histone deacetylases, histone demethylases (erasers); methyl-CpG binding domain proteins and chromodomain-containing proteins (readers) (5).

A highly observed phenomenon in most cancer cells is altered post-translational modification of histones caused by the dysregulation of epigenetic regulators, which ultimately alters chromatin structure (5-7). These post-translational modifications bear an important role in controlling the structure of the chromatin (Figure 1), which subsequently alters gene expression by remodeling the nucleosome structure to a condensed or loosened state, promoting gene repression or activation, respectively (6). This dysregulation was found to promote pro-proliferative and pro-survival gene transcription, and/or direct repression of pro-apoptotic and/or pro-differentiation proteins (5-7). Furthermore, oncogene transformation and tumorigenesis are mediated by epigenetic events that contribute to their development (5-9). For instance, hypermethylated DNA CpG islands and histone hypoacetylation/hypermethylation contribute to the repression of tumor suppressor genes (6,7,82). Histone modifications, which include acetylation and methylation, impact several cellular processes, such as gene expression, heterochromatin activation and DNA replication and repair (5-9). Histones (H) H2A, H2B, H3 and H4 make up the

basic structure of nucleosomes by forming a histone octamer (5). Histone modifications typically occur on the N-terminal tail of each of these histones, which protrudes outwards from the nucleosome (6). The N-terminal tail is abundant with lysine (K) and arginine residues, where several post-translational modifications of histones can occur (5-7).

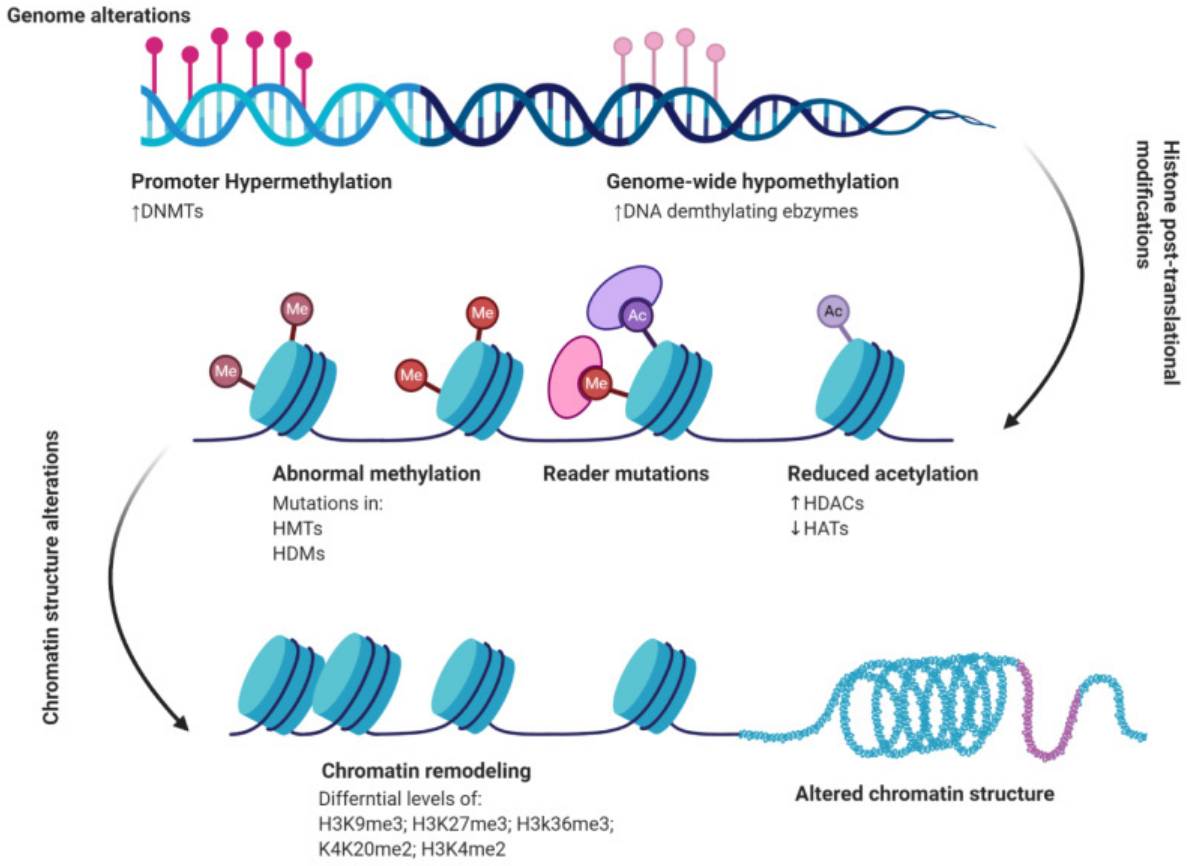

Figure 1. – Genomic alterations of chromatin by epigenetic regulators result in altered chromatin structure. Epigenetic regulators regulate gene expression by either adding or removing chemical groups directly on the DNA or on the N-terminal tails of histones. DNA epigenetic writers and erasers are DNMTs and DNA demethylating enzymes, which alter gene expression at the promoter or genome wide. Histone methyl or acetyl writers (HMTs, HATs) and erasers (HDMs, HDACs) add or remove chemical groups at specific residues present on the N-terminal tail of histones. These post-translational modifications can help induce chromatin remodeling by altering the distance between nucleosomes leading to an altered chromatin structure. Differential expression of these epigenetic regulators due to mutations

or overexpression further alters the chromatin structure possibly promoting oncogenesis (5-7). DNA methyltransferases, DNMTs; Histone methyltransferases, HMT; histone acetyltransferases, HAT; histone demethylases, HDMs; histone deacetylases, HDACs. Created with BioRender.com

1.1.2 Histone lysine methylation

The lysine residues of the N-terminal tail of histones can be methylated (8,9). More specifically, H3 can be methylated at K4, K9, K27 and K36, while K20 is an important target of methylation of H4 (8). Methylation of H3K4 and H3K36 is associated with gene activation, whereas methylation of H3K9, H4K20 and H3K27 is generally associated with gene repression (7,8). Consequently, the demethylation of these lysine residues affects gene transcription (8).

Altered histone methylation can contribute to carcinogenesis by an accumulation of repressive or active histone marks, which can occur following altered expression of methyl-associated writers and erasers or by the mutation of the histone marks (5,8,9). For instance, the onset of pediatric gliomas and sarcomas is promoted by H3K27M (lysine to methionine) and H3K36M (9,86). These mutations prevent the tri-methylation of H3K27 and H3K36, promoting the expression of proliferative genes and reducing the expression of differentiation genes (9). Differential expression of histone methylation writers and erasers have also been linked to carcinogenesis in different types of cancers; however, in the context of cancer, the most studied histone methylation epigenetic regulators are the erasers, also known as histone lysine demethylases (5,8,9,86))

There are two types of lysine demethylases: Flavin adenine dinucleotide-dependent amine oxidases and Fe(II) oxygenases (7). Amine oxidases demethylases can demethylate mono- and di-methyllysine residues but are unable to demethylate tri-methyllysine groups (7,8). Alternatively, Fe(II) oxygenase demethylases are not only efficient at demethylating mono- and di-methyllysine residues, but also tri-methyllysine residues (8). Consequently, Fe(II) oxygenase demethylases seem to have a wider range of targets and would have a greater impact on epigenetic regulation. Lysine demethylase 4 (KDM4) is a protein family of Fe(II) oxygenases that use Fe(II), O_2 and 2-oxoglutarate, also known as α-ketoglutarate (αKG), as co-substrates of the

enzymatic reaction. These demethylases are characterized by a Jumonji C (JmjC) domain which is responsible for the protein's enzymatic function (8,9). The KDM4 family consists of KMD4A-E, making it the largest JmjC-containing demethylase group (7-9). KDM4A, B and C are expressed in all human and mouse tissues, while KDM4D and E are mostly expressed in mouse testes (8,9). The KDM4 family also goes by the name of Jumonji C domain-containing 2 (JMJD2) family (9).

1.1.3 KDM4 protein family

The different members of the KDM4 family (Figure 2) have two conserved domains, JmjC and JmjN (7-10). As mentioned earlier the JmjC domain is responsible for the enzymatic activity of the proteins; however, it requires a constant interaction with the JmjN domain which provides the protein structural support (7). Only KDM4A, B and C have two plant homeodomains (PHD) and a Tandem Tudor (TT) Domain (8-10). The PHD and TT domains allow the proteins to acquire histone sequence reading capabilities (9,10). These domains impact the binding affinity of the KDM4 proteins to their substrates, ultimately affecting subsequent protein-protein interactions (7-10).

The members of the KDM4 family that have the PHD and TT domains can demethylate mostly di- and tri-methylated H3K9 and H3K36 and bind to di-and tri-methylated H3K4 and H4K20 (7-9). The latter interactions are non-catalytic (9). For instance, during the DNA damage response, KDM4A's TT domains bind to di-methylated H4K20, which competes with the binding of p53-binding protein 1 (53BP1), a critical DNA damage response factor (18). Furthermore, the degradation of KDM4A is needed to be able to orchestrate the DNA damage response (18). Another example of the non-catalytic binding role of the KDM4 family TT domains is the binding of KDM4A to di-methylated H3K4. H3K4 is an active promoter mark (7,8). Consequently, KDM4A's ability to bind to di-methylated H3K4 through its TT domains could inadvertently aid its catalytic activity to demethylate the repressive histone mark tri-methylated H3K9 (7).

Out of all the members of the KDM4 family, KDM4A, B and C seem to be differentially expressed in several types of cancers (8-9). This dysregulation results in increased proliferation, tumor survival and metastasis (7-9). KDM4A is overexpressed in cancers such as ovarian, squamous cell, colorectal, breast, prostate and lung cancer (8). KDM4B is overexpressed in breast, prostate

and colorectal cancer (8,9). Its overexpression is correlated with ER+ aggressive subtypes of breast cancer (9). KDM4C is overexpressed in different types of carcinomas and lymphomas (7-9).

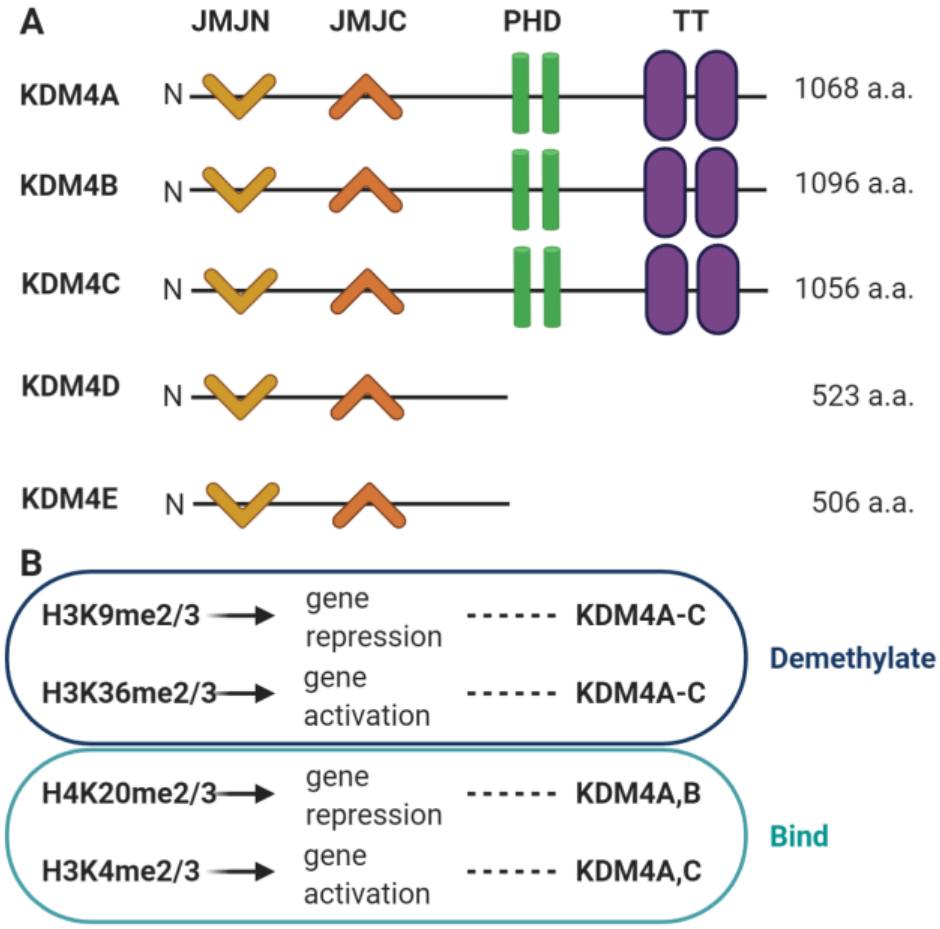

Figure 2. – A) KDM4 protein family schematic structure. JmjC is the catalytic domain. JmjN maintains structural integrity and sustains JmjC activity. Two PHD and TT domain provide stability and affinity of interaction to substrate. B) The main catalytic and binding substrates of KDM4 protein family. KDM4A-C are able to demethylate di- and tri-methyl H3K9/36. KDM4A and KDM4B bind H4K20 me2/3 while KDM4A and KDM4C H3K4 me2/3. Plant homeodomain, PHD; Tandem Tudor, TT; methyl, me. Created with BioRender.com

1.2 KDM4A

Out of the more prominent KDM4 proteins, KDM4A/JMJD2A is among the most studied (7-9,13,15). In breast and colorectal cancers, the loss of KDM4A is accompanied by a decrease in proliferation and a stalling between the G2/M-phase in the cell cycle (7). A similar proliferative profile can be observed when KDM4A is depleted in osteosarcoma cells, which also results in stalling in the cell cycle (7,87). KDM4A also interacts with transcription factor AP1, activating protein 1, which promotes tumorigenesis by inducing cell proliferation and cell growth (9). Additionally, AP1 controls apoptosis and differentiation by inducing the expression of genes that promote cell growth and metastasis (9,88). KDM4A further aids AP1 to bind to the promoters of its target genes, thus promoting their expression (9).

Consequently, KDM4A seems to play a role in tumor progression through the promotion of proliferation, which is a phenomenon that is intertwined with the progression and persistence of tumors (1-9). To better understand the role of KDM4A in carcinogenesis, the function of KDM4A in the different stages of cellular development and under different stress responses will further elaborated on. As mentioned earlier, KDM4A demethylates mostly di- and tri-methylated H3K9 and H3K36 (7-9). It can also affect the binding of transcription factors to their targets, which has a further impact on different cellular responses (8,9). It was found to play a role in the following cellular processes: development, replication, DNA damage, and senescence (8,9,11-13,18,25,26). The following are examples of the divergent yet important roles of KDM4A.

1.2.1 Development: KDM4A is important for female fertility

Embryonic development depends on proper oocyte fertilization and development into embryos, and their subsequent implantation into the uterine wall (11). A fertilized oocyte becomes an embryo, which develops into a blastocyst that contains inner cell mass and trophectoderm cells (11,89). The blastocyst will undergo structural changes, which allows its implantation into the uterine wall (11). Implantation is a multistep process that begins when the “window of implantation” is established. The window of implantation is characterized by a luteinizing hormone (LH) surge (11,89). The most noted spontaneous abortion in females is when the

implantation of the embryo occurs after the window of implantation (11). Implantation occurs in three stages; apposition, adhesion, and invasion. During the apposition stage, the surface of the blastocyst makes contact with the implantation site of the endometrium. Cell adhesion phase occurs when the blastocyst trophectoderm cells comes into contact with the luminal epithelium cells of the uterus (89). Finally, the blastocyst invades the endometrial stroma of the uterine wall and is implanted, which is also known as the invasion phase (11,89).

KDM4A is highly expressed in the female reproductive system; loss of KDM4A in mice causes female infertility, specifically because of KMD4A's important role in oocyte and pre-implantation development (12,90). KDM4A null mice have decreased levels of LH and prolactin, both of which have an important role in establishing pregnancy by promoting the window of implantation and ensuring pre-implantation, respectively (12). Additionally, KDM4A seems to regulate gene expression by binding to H3K4 tri-methyl abundant regions, whether in the promoter or intergenic regions, to decrease the amount of H3K9me3 (12,90).

Another aspect of the development process that seems to depend on the presence of KDM4A is differentiation of embryonic stem cells into vascular endothelial cells (13). In mice, KDM4A and KDM4C independently promote the expression of Flk1 and VE-cadherin, important mesodermal and vascular lineage markers (13,91). Early in the differentiation process, KDM4A demethylates H3K9 tri-methyl at the promoter region of Flk1. KDM4A expression is increased throughout all the stages of differentiation; however, KDM4C expression reaches its peak on the 5th day of the 6-day differentiation cycle. KDM4C further demethylates H3K9 tri-methyl at the promoter region of VE-cadherin. Depletion of either demethylase showed a significant decrease in differentiation (13).

1.2.2 Replication: KDM4A promotes chromatin accessibility prompting progression through S-phase

Three major steps outline DNA replication, the first being the assembly and activation of the pre-replicative complex, followed by the activation of replication, and finally culminating in DNA chain elongation (14). The assembly of the pre-replication complex begins after mitosis has taken place and continues throughout the G1-phase of the cell cycle (14,78). As the cell exits

mitosis, the origin of replication complex (ORC), which consists of ORC1-6, binds to the replication origins. In the G1-phase, cell division control protein 6 (CDC6) and chromatin licensing and DNA replication factor 1 (CDT1) recruit the minichromosome maintenance complex (MCM), which consists of MCM2-7, to the ORC-binding sites. The resulting complex is known as the pre-replicative complex, which is activated when MCM2-7 bind to the DNA (14). DNA replication occurs during the S-phase, when CDKs and Dbf4-dependent kinase (DDK) phosphorylate the key components that eventually lead to the activation of the replicative helicase (14,78). The access of the pre-replication complex to the replication origin is mediated by chromatin remodelers known as SWI/SNF. These remodelers coordinate nucleosome spacing with the help of epigenetic erasers, eventually altering chromatin structure (14).

Furthermore, chromatin structure has a strong impact on the initiation of the process of DNA replication (14,15). Since the chromatin structure is altered through DNA and histone modifications, irregularities in these modifications can prevent the expression of tumor suppressors (2-5). Additionally, the more available DNA regions caused by an open chromatin structure are more readily replicated during the cell cycle (5). Evidence has shown that KDM4A is overexpressed throughout the stages of the S-phase. In addition, a greater quantity of open chromatin areas was observed in KDM4A-overexpressing cells (15). Cells that overexpress KDM4A move into late S-phase faster than those expressing endogenous levels of KDM4A. Moreover, the expression of KDM4A during the early and late stages of the S-phase presents the notion that KDM4A plays an important role in DNA accessibility through the promotion of an open chromatin structure (7-9,15). To further reiterate this notion, an assay detecting BrdU incorporation highlighted an H3K9 tri-methyl dependent activity in KDM4A's replication role. In other words, chromosome 1 satellite 2 DNA (sat2), which is a region characterized by enrichment in H3K9 tri-methyl, was more accessible in KDM4A-overexpressing cells. Sat2 is a highly repetitive sequence found within heterochromatin. In *C. elegans*, KDM4A was shown to be important for the replication process as well as for the replication timing (15).

1.2.3 DNA Damage Response: KDM4A degradation necessary for non-homologous end-joining repair

Damage to the DNA may occur in different forms; base deletion, adducts formation, single-stranded breaks (SSBs), and double-strand breaks (DSBs) (16,78,81). These events can occur through the dysfunction of normal cellular processes, such as DNA mismatches during replication and failed enzymatic reactions of topoisomerases or by-products of oxidative respiration. Exogenous stresses, however, are also able to highly damage DNA. For instance ionizing radiation causes DSBs, the most toxic form of DNA damage. The DNA damage response (DDR) identifies these lesions and promotes their repair (16).

DSB repair consists of two pathways, homologous repair (HR) and non-homologous end-joining (NHEJ) (16,17). HR requires a sister-chromatid sequence as template to mediate repair and thus occurs only in S- and G2-phases. This pathway is initiated when MRE11/Rad50/NBS1 (MRN) protein complex binds a DSB (17). The MRN complex will then hold the break together and allow for the subsequent binding of CtIP nuclease to form the MRN-CtIP complex, which interacts with exonuclease I to resection the end of the break. The resulting sequence will be molded into homologous DNA by RPA and RAD51 nucleoprotein filaments to form a temporary triplex-DNA structure. At this point, strand exchange will occur to repair the break (17). Conversely, NHEJ occurs in post-mitotic and G1-phase cells. The breaks are recognized by Ku70/Ku80 proteins hetero-dimer, which in turn activate Phosphoinositide 3-kinase (PI3K) (17,18). The kinase then allows for the recruitment of the Artemis nuclease and the MRN protein complex (17).

The MRN complex promotes the activation of ATM kinase that phosphorylates H2AX (γH2AX) at K139 residues (18,19). The accumulation of γH2AX recruits RING finger protein (RNF) 8 and RNF168 E3-ubiquitin ligases (18). These ligases form polyubiquitin chains on histones at K63 at the DSB, and are responsible for the localization and stabilization of mediator proteins, 53BPI and breast cancer-associated gene 1 (BRCA1), onto the DNA damage site (17,18). Cells with DSBs are able to choose the appropriate repair pathway with the help of these mediator proteins. While 53BPI promotes the NHEJ pathway, BRCA1 promotes the HR pathway. H4K16

acetylation promotes BRCA1 recruitment to the site of DSB (17). In contrast, 53BPI, similar to KDM4A, can bind to H4K20 di-methyl through its TT domain (18). Mutations or abnormal expression of these proteins was shown to impair DDR and cause genome instability. Dysregulation of these enzymes was also shown to promote tumor occurrence and development (18,19).

The antagonizing binding activity between KDM4A and 53BPI can impact cell fate depending on the circumstance, depicted here in Figure 3 (18). KDM4A binds tightly to H4K20 di-methyl and must therefore be removed to allow for 53BPI binding and the formation of 53BPI foci at DNA damage sites. Furthermore, it was found that KDM4A was degraded following DNA damage in an RNF8 and RNF168 ubiquitin ligase-dependent manner. Consequently, KDM4A degradation during DNA damage response not only makes room for 53BPI binding to H4K20 di-methyl, but also stabilizes the amount of available H3K36 di-methyl. These histone marks promote the recruitment of DNA damage repair factors such as the MRN complex subunit, NBS1, which promotes H2AX phosphorylation (18).

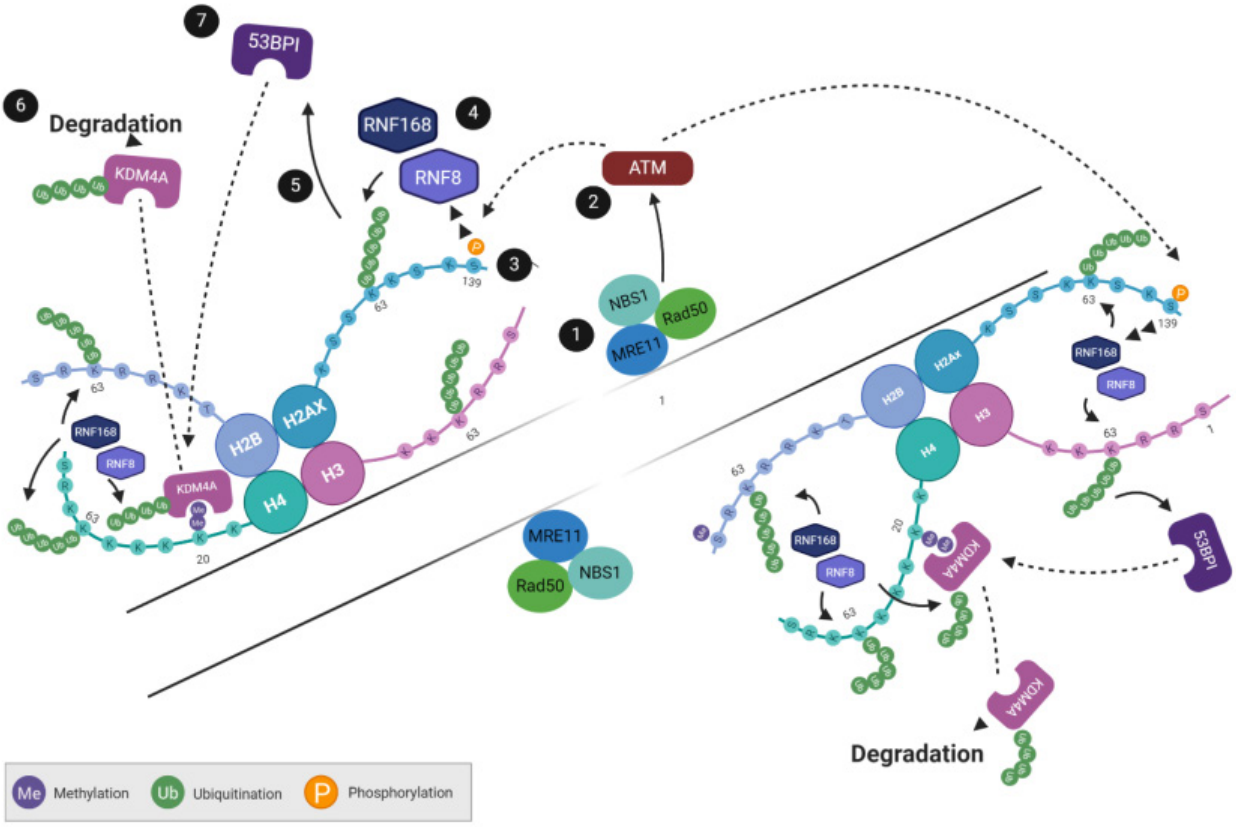

Figure 3. – Recognition and initiation of DSB repair. 1) The MRN complex recognizes and binds to the DSB. 2) ATM kinase is recruited to the DNA damage site and 3) proceeds to phosphorylate H2AX at K139. 4) RNF8/168 ligases recognize γH2AX and add polyubiquitin chains on K63 residues of histones. 5) These chains promote localization of 53BPI to the DSB. 6) RNF8/168 ligases also form polyubiquitin chains on H4K20me2-bound KDM4A, which promote its degradation. 7) 53BPI is then able to bind to the free H4K20me2 and initiate NHEJ repair pathway. Created with BioRender.com

1.2.4 Cellular Senescence: KDM4A hinders the induction of cellular senescence

Cellular senescence, which is the process by which a cell goes into a growth arrest in response to stress (20).This process was first tied to ageing in a phenomenon called replicative senescence; however, new evidence shows that different stresses cause senescence, such as oncogene activation, DNA damage response, and epigenetic stressors (20-26). Once the cell is

subjected to such stresses, ATM/ATR kinases contribute to the stabilization of p53 protein, which induces the transcription of p21, resulting in cyclin E–CDK2 inhibition (20). Another prominent pathway that induces cellular senescence is the inhibition of c-myc, which activates the p16 pathway (20,23). Activated p16 will then inhibit cyclin D–CDK4/6 complexes. Both the p53 and p16 pathways can occur at the same time or can be induced separately. Under normal conditions, the cyclin complexes that are inhibited by p21 and p16 help progress the cell cycle by inhibiting pRB. Consequently, p21 and p16 promote cell cycle arrest by preventing the inhibition of pRB, which in turn prevents the expression of E2F target genes that are responsible for S-phase progression. The cells then either undergo repair, stress relief, senescence, or apoptosis (20). If the stress is severe, then the cells will undergo senescence and start secreting pro-inflammatory factors, such as cytokines, growth factors, and proteases. The secretion of these factors is also known as senescence-associated secretory phenotype (SASP) (23). Early senescent cells that have been induced through an oncogene-activated stress could become non-senescent by PI3K activation; however, most early senescent cells will eventually undergo immunoclearance (20,23).

1.2.4.1 Oncogene-induced senescence

Oncogene-induced senescence (OIS) is brought upon by upregulation of oncogenes such as RAS and by downregulation of tumor suppressors such as p53 and PTEN (21,30). Hyper-activation of oncogenes causes replicative stress that results in DNA damage (21,92). It was shown that inhibition of DDR proteins, such ATM, abolishes OIS, indicating that DNA damage response is an important mediator of OIS (21). Consequently, mutations or loss of DDR proteins can prevent the onset of OIS and furthermore promote carcinogenesis (21,92).

1.2.4.2 Senescence and cancer

Senescent cells undergo a stable growth arrest. These cells stop responding to mitogen signaling and consequently stop proliferating (20-22). Consequently, this could be a way of blocking the progression of tumor cells, which have a high proliferative profile. As such, triggering senescence should be able to slow down if not halt the proliferative capacity of tumor cells (22). Senescent tumor cells could then be eliminated by the immune system (20,23). The activation of

tumor suppressor p53 promotes the tumor to secrete chemokines that lead to the recruitment of Natural Killer cells (NK). NK cells would subsequently promote the elimination of the senescent tumor cells (22).

Alternatively, it has been shown that senescent tumor cells can revert and become proliferative cells (24,64). SASP can, in some cases, promote tumor progression response by providing the optimal tumor microenvironment (65). It has been found that senescence induction does not necessarily induce SASP formation (23). Senescent fibroblasts were shown to promote tumorigenesis by independently inducing SASP molecules such as Osteopontin (OPN), IL-6, and IL-8. More specifically, OPN was found to be overexpressed in all stages of tumorigenesis. Upon senescence stimuli induction, OPN is expressed through the induction of NF-κB and ATM signalling pathways. Its expression is then upregulated by a dominant-negative form of histone deacetylase 1 (HDAC1), which is a chromatin remodelling agent (23).

In addition, it was found that, in head and neck squamous cell carcinoma, Fragile X-related protein 1 (FXR1) provided the opportunity for tumor cells to bypass senescence (24). FXRI was found to bind to the mRNA of p21 and TERC, which are cell cycle regulators known for their important roles in maintaining the senescence phenotype and telomerase activity, respectively. It was found to destabilize p21 RNA while stabilizing TERC mRNA. This not only allows for the disruption of p53-dependent senescence, but also promotes cell immortality (24,64).

1.2.4.3 Senescence and KDM4A

KDM4A was found to hinder the induction of senescence in the context of cancer where cellular senescence is considered as a tumor suppressor response (20,92). KDM4A was found to be degraded by miR-137, which is miRNA that plays a role in the induction of senescence (92). Furthermore, overexpression of KDM4A promoted a bypass of miR-137 induced senescence through downregulation of p53 and pRB tumor suppressors (92,25). It was also found that KDM4A promotes the transcriptional repression of tumor suppressor gene chromodomain helicase DNA-binding domain 5 (CHD5) (26). The downregulation of CHD5 affects the progression of cellular senescence by impacting the activation of the p53 pathway, which is important for the progression of OIS (25,26). In certain contexts, inhibiting the p53 pathway is

enough to halt the progression of senescence. In the context of lung cancer, KDM4A was found to be an oncogene that when overexpressed promotes the transcriptional repression of CHD5. This impacts OIS by negatively regulating the p53 pathway (26). KDM4A was also found to interact with HDAC1, which promotes the bypass of senescence, as previously discussed (23). Most importantly, KDM4A depletion was efficient at triggering Ras-induced senescence in lung cancer, making it a novel therapeutic target (26).

The proteins that have previously been found to interact with KDM4A are summarized in Table 1.

Tableau 1. – List of KDM4A validated interacting proteins and their function adapted from (7,9,18,23,31,32,51-55)

Interacting protein	***Annotation***	***Function***	***References***
H3	Histone	Structure of chromatin	Berry WL *et al.*, 2013
H4	Histone	Structure of chromatin	Berry WL *et al.*, 2013
H1.4	Histone	Structure of chromatin	Berry WL *et al.*, 2013
AP1	Tumor suppressor	Controls cell proliferation, apoptosis and differentiation	Labbe RM *et al.*, 2013
RNF168	E3 ubiquitin ligase	Adds polyubiquitin chain on K63 of histones surrounding DNA damage site; Adds polyubiquitin chain on KDM4A for degradation	Mallette FA *et al.*, 2012
RNF8	E3 ubiquitin ligase	Adds polyubiquitin chain on K63 of histones surrounding DNA damage site; Adds polyubiquitin chain on KDM4A for degradation	Mallette FA *et al.*, 2012
HDAC1	Chromatin remodelling agent	Aids in the bypass of senescence	Pazolli *et al.*, 2012

USP1	Deubiquitinase	Deubiquitinates key proteins that play a role in cellular processes such as differentiation and DNA repair	Cui SZ *et al.*, 2020
SCF^{FBXO22}	E3 ubiquitin ligase	Targets KDM4A for degradation	Tan MK *et al.*, 2011
E2F1	Transcription factor	Cell cycle gene transcription activator and binds to pRB; mediates cell proliferation.	Wang LY *et al.*, 2016
ETV1	Transcription factor	Controls expression of genes involved in cell proliferation, cell growth and differentiation	KIM TD *et al.*, 2011
NCOR1	Transcriptional corepressor	Interacts with HDAC to prevent transcription of genes such as p21 and ASCL2	Wang J *et al.*, 2016
pRB	Tumor suppressor	Regulator of the cell cycle; responsible for the progression of the cell cycle	Gray SG *et al.*, 2005
p53	Tumor suppressor	Regulator of cell cycle; responsible for the prevention of formation of tumors; plays a role in DDR and senescence	Kim T-D *et al.*, 2012

1.3 KDM4A and cancer

KDM4A contributes to carcinogenesis by association to different cellular pathways that promote cell proliferation. In several cancer models, inhibition of KDM4A was found to decrease cell proliferation as well as, in some cases, tumor size (4,27,29,32-35). Copy number variation is one of the hallmarks of cancer, and is characterized by the gain or loss of genomic regions, chromosome arms and/or chromosomes (27). This generally occurs in the S-phase, in which

KDM4A is upregulated (15). Furthermore, KDM4A was found to contribute to tumorigenesis by increasing gene copy number at specific sites (8,27). Overexpression of KDM4A results in more available regions in the chromatin, allowing for an increase in copy number variation. More specifically, KDM4A increases the copy number of 1q12, 1q21, and Xq13.1, which are site of putative oncogenes (27). These sites are also often amplified in cancers such as lung caner and multiple myeloma (8). Within 24 hours of KDM4A overexpression, the methylation pattern of H3K9/K36 was altered and a clear increase in copy number at region 1q12 was observed. Copy number gain at 1q12 was correlated with drug resistance in ovarian cancer and multiple myeloma cell lines (8). Consequently, copy number gain could ultimately highlight how KDM4A is contributing to cancers that are characterized by KDM4A upregulation (27).

Another way in which KDM4A contributes to carcinogenesis is through its impact on the AKT-mTOR pathways (28,29). The AKT-mTOR pathway promotes cell growth and proliferation and is activated by certain growth factors, such as insulin-like growth factor-1 and epidermal/endothelial growth receptors (30,93). These growth factors are recognized by cell membrane growth factor receptors tyrosine kinases, which autophosphorylate and activate PI3K. At this point, a series of downstream phosphorylations recruit essential signalling proteins, such as AKT to activate the mammalian target of rapamycin (mTOR) pathway. The mTOR pathway consists of two complexes, mTORC1 and mTORC2, which are sensitive to rapamycin and negatively regulated by PI3,4,5-P3, PTEN (30). Another negative regulator of the mTOR pathway is DEP domain-containing mTOR-interacting protein (DEPTOR) (28). In opposition to the oncogenicity of KDM4A described thus far, it has been found that it stabilizes DEPTOR and promotes the inhibition of mTOR activity (28,94). This occurs when mutations of the TCA cycle proteins isocitrate dehydrogenases 1 and 2 (IDH1/2) result in their ability to catalyze the conversion of αKG, one of the co-substrates required for KDM4A activity, into R-2-hydroxyglutarate (2HG). The structural similarity between 2HG and αKG allows 2HG to bind and inhibit KDM4A. In these cases, DEPTOR is no longer stable and can be subjected to proteolytic degradation. IDH1/2 mutations are highly present in low-grade gliomas and are independent of PTEN mutations, which are correlated with abnormal activation of the mTOR pathway in multiple cancers (28).

In high-grade gliomas, where the abrogation of PTEN promotes the hyper-activation of the mTOR signalling pathway, KDM4A is overexpressed (29). In contrast with KDM4A's function in low-grade gliomas, its knockdown seems to decrease the size of glioma tumors (28,29). Furthermore, KDM4A was found to promote cell proliferation by binding to the promoter site of Phosphoinositide-dependent kinase-1 (PDK1) and promoting its transcription through H3K9 tri-methyl demethylation (29). PDK1 contributes to the initiation of the mTOR pathway by activating AKT through its phosphorylation at threonine 308 (28,29). Additionally, once the mTOR signalling pathway was inhibited by rapamycin, KDM4A overexpression did not seem to affect cell proliferation, promoting the notion that KDM4A contributes to the increase in cell proliferation present in high-grade gliomas through a PDK1/AKT/mTOR pathway dependent manner (29). Furthermore, the contribution of KDM4A to cancer is still not completely clear and may be context dependent (28,29).

PTEN loss is also common in prostate cancer, in which KDM4A was also found to be overexpressed (31,32,95). In prostate cancer, the transcription factor androgen receptor (AR) plays a key role in tumorigenesis initiation and progression (31,32,96). AR promotes tumorigenesis with the help of AR-coactivators and corepressors (96). KDM4A is an AR co-activator that promotes the demethylation of H3K9 or H3K36 tri-methyl at gene promoters (31,32). For instance, KDM4A was found to recruit AR to the c-Myc enhance through the demethylation of H3K9 di-methyl at the enhancer site. The stability of KDM4A, however, was dependent on the activity of deubiquitinase USP1, which seems to stabilize KDM4A by deubiquitinating and preventing its degradation (31). Under normal conditions, the abundance of KDM4A is regulated by SCFFBXO22 ubiquitin ligase complex through its ubiquitination at K48, which promotes proteasomal degradation (32). Furthermore, USP1 stabilizes KDM4A by deubiquitinating K48 (31,32).

1.3.1 KDM4A and cervical cancer

HeLa cells are positive for human papillomavirus (HPV) (37,97). These cells originate from the patient Henrietta Lacks, who was diagnosed with adenocarcinoma of the cervix, which affects the glandular cells (98). HPV viral proteins E6 and E7 seem to promote tumorigenesis by

dysregulating p53 and pRB tumor suppressor pathways. It was also found that E6 and E7 modulate histone modification enzymes (37).

Detection and treatment of cervical cancer have improved greatly over the years; however, the survival rate greatly diminishes with delayed detection (38,39). Furthermore, more efficient treatment is required to combat a more established type of cervical cancer. During cancer development, tumor suppressors downregulate the proliferation pathways that are exploited by tumorigenic cells (21,22,26,30). MicroRNA (miR)-491-5p is a characterized tumor suppressor which was found to promote apoptosis and inhibit proliferation (35,99). In cervical cancer, KDM4A was found to be highly upregulated and correlated with bad prognosis (33-35). KDM4A was found to inhibit this tumor suppressor and tumors characterized by the overexpression of KDM4A expressed a decrease in pro-apoptotic proteins, such as Bax, p21 and active caspase-3, and an increase in anti-apoptotic protein Bcl-2. Consequently, the overexpression of KDM4A inhibited apoptosis, which was reverted by its knockdown. Additionally, KDM4A overexpression was found to induce tumor growth *in vivo* when compared to KDM4A knockdown mice (35).

Furthermore, KDM4A seems to play a crucial role in the maintenance of tumorigenesis in cervical cancer (31-35). This prompted us to chose cervical cancer as our model especially due to the evidence that the downregulation of KDM4A causes a decrease in tumor size and a decrease in proliferation in cervical cancer (33-35). Consequently, we aim to understand the role that KDM4A plays in cervical cancer by identifying its protein interactome.

Additionally, KDM4A is being currently investigated, along with its other dominant family members, as a novel epigenetic target for cancer therapy (36). Consequently, mapping the protein interactome of KDM4A could provide much-needed information for the use of these therapeutic agents. Better understanding the interacting partners of KDM4A in cervical cancer will not only elucidate the role of KDM4A in oncogenesis but can also help in improving treatment specificity. Furthermore, we will be identifying the protein interactome of KDM4A using a novel technique known as proximity-dependent biotin identification (BioID). The cell line used is the human HeLa cell line, which is a cervical cancer cell line (33-35).

1.4 BioID

BioID is a method that employs a promiscuous biotin ligase, BirA (40-43,68). When fused with the protein of interest, also known as the bait protein, BirA can biotinylate in the presence of biotin, directly interacting proteins or indirectly interacting proteins (40). These prey proteins are then pulled down by a streptavidin column and analyzed by mass spectrometry (MS) (40-43). The main advantage and difference between BioID and other affinity purification techniques is the ability to entrap the prey proteins in situ. However, the labelling radius is limited to <20nm. This method was successful *in vivo* as well *in vitro* making it an optimal technique in proteomics (40).

One of the main disadvantages of this method is the size of BirA (40,41). BirA was originally isolated from *E. coli*. It is 7.8 nm wide and 3.0 nm high (41). One way to resolve this issue is to prepare two constructs of the bait protein, one with BirA at the N- terminal and the other with BirA at the C-terminal, to prevent the loss of potential protein interactions. However, if the bait protein is small, then the size of BirA would prove to be a more serious problem. *A. aeolicus*, on the other hand, has a much smaller biotin ligase, currently known as BirA2, which is 3.8 nm wide and 3.0 nm high (41). Furthermore, BirA2 was proven to be as efficient at biotinylating prey proteins as BirA and the BioID analysis that uses BirA2 is known as BioID2 (40-43).

Ascorbate peroxidase (APEX) and horseradish peroxidase (HRP) are other ligases that can perform the same function as BirA (41-43). While BirA's activity may take from a few hours to a day (41,43), APEX and HRP can take only minutes to biotinylate a substantial amount of proteins (42). If the goal is to discover intermittent interactions following the initiation of a process, then APEX or HRP would be optimal (42). However, given that our aim is to find the protein interactome in an ongoing situation, BirA seems like the optimal ligase (41,42).

The BioID is best described by Paymen et al. (43). The bait protein, in this case KDM4A, is incorporated in Tetracycline (TET)- inducible lentiviral vector encoding BirA-flag either at the N- or C-terminal (42,43). There are five BioID TET-inducible vectors, pSTV2, pSTVH5, pSTV6, pSTVH7, and pSTVH8, each having Woodchuck Hepatitis Virus Posttranscriptional Regulatory Element (WPRE) and a Tetracycline response element, P-tight, with a CMV promoter. pSTVH5,

pSTV6 and pSTVH7 harbour selection markers, while pSTV2 and pSTVH8 do not. Additionally, these plasmids incorporate differing ORF sizes and only STV2 can sustain an ORF as long as KDM4A. Consequently, KDM4A infected cells do not have a selection marker. In addition, the cells must be infected with a separate lentiviral vector that encodes rtTA, which binds to P-tight and initiates gene expression upon the presence of TET or TET-like compounds, such as doxycycline (DOX), since only pSTVH5, pSTV6 and pSTVH8 encode rtTA (43).

There are many advantages to using lentiviral vectors (67,68). For instance, lentiviruses can infect dividing and non-dividing cells. Consequently, lentiviruses are highly efficient at infecting primary cells. In addition, they result in good expression levels (67). In this study, the expression levels can be controlled since the lentiviral vectors are TET inducible (43). This allows for the measurement of the direct genetic effect of KDM4A in HeLa cells since constitutive expression could generate false positives (68).

The optimal controls for BioID are BirA-EGFP and BirA-EGFP fused with a SV40 nuclear localization signal (NLS) (43). KDM4A is mostly a nuclear protein, consequently, GFPNLS and KDM4A share the same subcellular localization promoting an increase in specificity by more efficiently eliminating nonspecific interactions (7-10). Nonetheless, there is some cytoplasmic expression of KDM4A, which also makes BirA-EGFP and optimal promoter since it is expression at both cytoplasmic and nuclear levels (66).

Cells expressing the lentiviral pSTV2 vector harbouring the bait or control proteins are incubated in media containing up to 1µg/mL of doxycycline and 50µM of biotin and biotinylation occur over a period of 24 hours, *in situ* (43). The cells are then lysed and passed through a streptavidin affinity column. The collected biotinylated proteins are then identified through MS and the proximity partners are identified and ranked according to the statistical significance of their interaction with the bait using SAINTexpress statistical software (Figure 4). Finally, to insure reproducibility of the results, two biological replicates of each BioID experiment are required. The replicates must be infected and harvested on different dates (43).

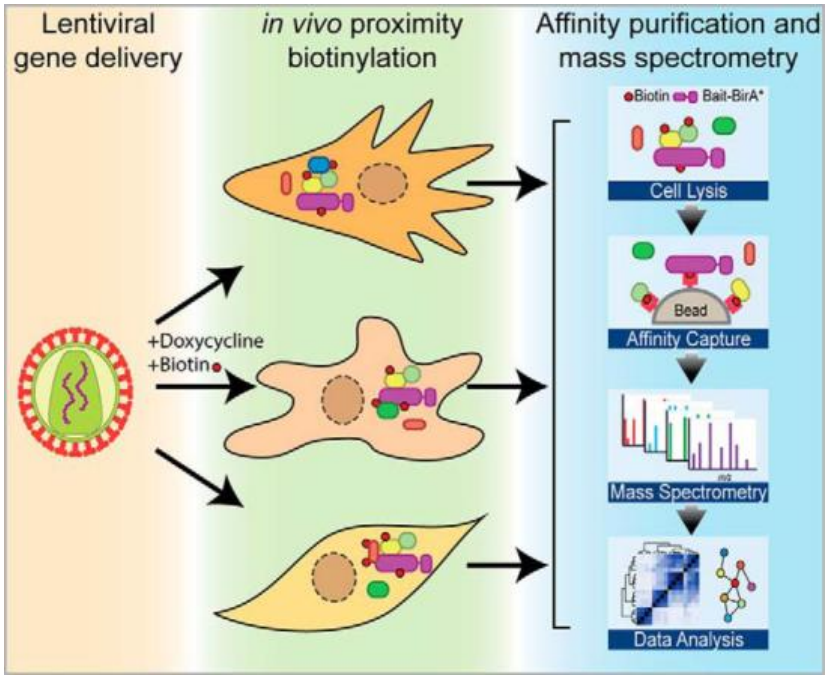

Figure 4. – Graphical representation of the BioID process. Adapted from Samavarchi-Tehrani et al. (43); see text for further elaboration.

1.5 Hypothesis and objectives

Given the role of KDM4A in differential gene expression during oncogenesis (7,8), we hypothesize that KDM4A interacts with chromatin remodelers and other transcription factors to promote carcinogenesis by altering gene expression in cervical cancer. To achieve this, we have set two objects, the first is to identify the protein interactome of KDM4A using BioID2, which utilizes BirA2 (42). The second objective is to validate the results using streptavidin pull down. We intend on comparing partners of KDM4A with those of the catalytic dead mutant KDM4A^{H188A} and the TT mutant KDM4A-ΔTT. The KDM4A-ΔTT lacks the TT domain that ranges 897-1011 amino acids. This will allow us to determine the interactions that are associated with or dependent on the catalytic activity and the TT domain of KDM4A.

Chapter 2 – Materials and Methods

2.1 BioID2 expression plasmid construction

The first step to perform the BioID2 experiment is to construct the pSTV2 plasmid containing both BirA2 at the N-terminal or the C-terminal of KDM4A, the catalytic down mutant KDM4A^{H188A}, and the TT mutant KDM4A-ΔTT. The cloning was carried out using the Gateway® technique. The entry clone was generated using restriction cloning and then recombined, using LR recombination, into the expression plasmid pSTV2 to form pSVT2.BirA2-KDM4A/H188A/TT and pSVT2.KDM4A/H188A/TT-BirA2. Finally the plasmids were expressed in HeLa cells. The plasmids *pSTV2.*BirA-EGFP and pSTV2.BirA-EGFP-NLS were kind gifts of Dr. Anne-Claude Gingras, PhD.

2.1.1 Restriction cloning

Restriction enzymes are used to create sticky ends on the gene and the plasmid. This allows the gene to ligate to the plasmid. The plasmid is then transformed into bacterial competent cells. Single bacterial colonies are picked and grown in liquid culture. When the bacterial growth is still at the exponential phase, the competent cells are collected and the DNA plasmid is purified and sequenced.

2.1.1.1 Generating PCR product with sticky ends

The bait in the BioID experiment is fused to BirA2 at its N- or C-terminal, consequently, the bait should not harbor a start or a stop codon depending on the position of BirA2, N- or C-terminal respectively. Furthermore, a PCR product of KDM4A and its mutants was generated lacking either a start or a stop codon. In addition, two restriction sites (RI) were added at the N- and C-terminals of the genes; NOTI RI at the N-terminal and ASCI RI at the C-terminal. These sites are also present in the multiple cloning site of the Gateway® ENTRY plasmid, pENTR.

The primers used to generate the PCR products are summarized in Table 2. KDM4A and KDM4A^{H188A} were already in the laboratory plasmid directory, but KDM4A-TT mutant needed to be generated using inverse PCR. Briefly, 10 to 100 ng/µl of plasmid DNA was amplified using 0.5µl of Q5® High-Fidelity DNA Polymerase (M0491, New England Biolabs Inc.), 10 mM dNTP, 10µM primers and 5x Q5 reaction and enhancer buffer in a volume of 25µl. The DNA was initially denatured at 95°C for 5 minutes, then went through 30 cycles of denaturing (95°C for 30 seconds), annealing (60°C for 60 seconds) and extending (72°C for 120 seconds). After the completion of the cycles, the product was subject to another 8 minutes of extension at 72°C and held at 4°C until removal. The PCR product length was then verified on agarose gel. The length of KDM4A and KDM4A^{H188A} is 3192bp. Note the PCR reaction negative control has dH_2O replacing DNA. The PCR product is then purified using Monarch® PCR & DNA Cleanup Kit (5µg) (New England Biolabs Inc.)

2.1.1.2 Inserting PCR product into entry plasmid pENTR

The PCR products and pENTR plasmid were digested with NOTI (R3189L, New England Biolabs Inc.) and ASCI (R0558L, New England Biolabs Inc bs) 4U enzyme/1µg DNA for 15 minutes at 37°C followed by 1µl of CIP for 1 hour at 37°C to remove phosphate groups and prevent the annealing of the plasmid onto itself. The digested DNA and plasmid are then run on a 0.8% agarose gel, and extracted from the gel using Monarch® DNA Gel Extraction Kit (New England Biolabs Inc). The concertation of the digested plasmid and PCR products was measured using Tecan Infinite® 200 PRO (Trading AG).

The digested plasmid and PCR products produced sticky ends that facilitate their ligation. The following equation was used to calculate the ng of PCR product to be used in the ligation process: ng insert = (ng vector x molecular weight (kb) of insert / molecular weight (kb) of vector) x3. Furthermore, the molecular weight of pENTR and KDM4A are approximately 2.6 kb and 3.2 kb, respectively. For 50ng of pENTR, a maximum of approximately 185ng of KDM4A PCR product must be used for ligation. The ligation was carried out at room temperature for 1 hour by 1µl T4 DNA ligase enzyme in a 20µl reaction containing 50ng of digested pENTR and 185ng of digested KDM4A/KDM4A^{H188A} with or without start/stop. The negative control of the ligation reaction has dH_2O replacing the insert DNA. The ligation product was then verified on gel.

The ligation products were then transformed into Mach1 T1R chemically competent cells (ThermoFisher Scientific Inc.). 50µl of Mach1 cells were transformed with up to 12µl of ligation reaction. The competent cells/ligation mix incubated on ice for 15 minutes and then at 42˚C for 2 minutes. This was followed by another incubation on ice for 10 minutes. 400µl of LB liquid media was added to the competent cells/ligation mix, which was then incubated at 37˚C for 1 hour. 150µl of the mix was plated on kanamycin containing (KAN+) LB agar and incubated overnight at 37˚C. The ligation reaction negative control was also plated as competent cells of the negative control ligation reaction will not be able to grow KAN+ LB agar.

The next day, 2 to 3 clones were isolated/colony and pre-cultured in 5mL of KAN+ LB agar. Note that the working concentration of KAN is 50µg/mL. The pre-cultures were then incubated overnight at 37˚C whilst shaking at minimum 150 rpm. The following day, the DNA was extracted using Monarch® Plasmid Miniprep Kit (New England Biolabs Inc). The extracted DNA is then sequenced with M13F/R and KDM4A_seq primers (Table 2). Another form of ligation conformation was done by single digestion of the plasmid at RI site of BstZ17I RI enzyme (R05945, New England Biolabs Inc.) resulting in a blunt end at 3009bp of KDM4A. 1U of enzyme is sufficient to 1µg of DNA in 1 hour at 37˚C.

The resulting plasmids are pENTR.KDM4A w/o start codon, pENTR.KDM4AA w/o stop codon, pENTR.KDM4A^{H188A} w/o start codon, and pENTR.KDM4A^{H188A} w/o stop codon.

2.1.1.3 Generating KDM4A-TT mutant

The plasmids pENTR.BirA-KDM4A and pENTR.KDM4A-BirA were used as templates for the inverse PCR reaction generating the TT domain deletion. More specifically, the Tudor 1 and Tudor, which ranges from 897-1011 amino acids and make up the TT domain (9), were deleted. The PCR reaction followed the recommended Q5® High-Fidelity DNA Polymerase protocol (New England Biolabs Inc.) Briefly, the initial denaturing step was 30 seconds at 98˚C followed by 30 cycles of denaturing (98˚C for 10 seconds), primer annealing (68˚C for 30 seconds) and strand extension (20seconds/kb). The negative control for the PCR reactions had no DNA. The resulting plasmids pENTR.KDM4A-TT w/o start codon and pENTR.KDM4A-TT w/o stop codon are 6045bp, which run on gel to confirm the size.

The linear plasmid is then ligated by using T4 Polynucleotide Kinase enzyme (M0201, New England Biolabs Inc.), which phosphorylates DNA at the 5' for ligation, which is carried by T4 DNA ligase (M0202, New England Biolabs Inc.). Briefly, 2µL of the PCR reactions were incubated separately with 0.5µL T4 DNA ligase and 0.5µL T4 PNK in 20µL solution containing 1X T4 DNA ligase buffer (M0202, New England Biolabs Inc.). The reaction was carried out at 37˚C for 1 hour. 5µl of the ligation reaction were taken to perform DPNI digestion, which removes the methylated parental DNA template. The 20µL reaction was performed at 37˚C for 1 hour using 10x cut smart buffer and 1µL of DPNI (R0176, New England Biolabs Inc.). The control of the DPNI digestion are the reactions w/o DPNI. The resulting solution was then transformed in Mach1 competent cells as explained earlier. The -DPNI reaction KAN+ LB agar dishes must have more colonies than the +DPNI reaction KAN+ LB agar dishes. Colonies were picked, pre-cultures and sequenced as described above. The plasmids were also digested with NOTI and BstZ17I RI enzymes.

The resulting plasmids are pENTR.KDM4A-TT w/o start codon and pENTR.KDM4A-TT w/o stop codon.

2.2 Generation of expression clones for BioID assay

The gene of interest is recombined into the expression vector, pSTV2, through the LR recombination reaction using Gateway® LR Clonase® II enzyme by following the protocol provided by ThermoFisher Scientific Inc. (Document Part Number 250522; Publication Number MAN0000282). In short, in an 8µL reaction add 50-150ng of the entry clone, 150ng/ of destination vector pSTV2 and TE buffer pH 8.0. 100 ng (2 µL) of pENTR™-gus was used as a positive control. To each reaction of 2 µL of LR Clonase® II enzyme mix was added and mixed well by vortexing. The samples were then incubated at 25°C for 1 hour. Finally, 1 µL of the Proteinase K solution was added to each sample to terminate the reaction, which were subsequently incubated at 37°C for 10 minutes. Next, 1 µL of each LR reaction was transformed into 50 µL of phage resistant STBL3 competent cells. The samples were then incubated on ice for 30 minutes followed by 42 seconds incubation at 42°C. This heat shock allows the DNA to be

introduced into the competent cell. 250µL of LB liquid medium was added to each sample, which were then incubate at 37°C for 1 hour with shaking at 225 rpm.

Following incubation, 100 µL of each transformation samples was plated onto LAB agar dishes containing 100 µg/mL ampicillin (AMP) and incubated at 37˚C overnight. The next day, the samples were extracted using Monarch® Plasmid Miniprep Kit (New England Biolabs Inc.) and sequenced using LNCX and WPRE primer (Table 2). LNCX forward primer was used for samples having BirA at the C-terminal, while WPRE reverse primer was used for samples having BirA at the N-terminal. The plasmids were also digested with NOTI and BstZ17I RI enzymes.

The resulting plasmids are pSTV2.flag.BirA-KDM4A, pSTV2.KDM4A-BirA.flag, pSTV2.flag.BirA-KDM4A^{H188A}, pSTV2.KDM4A^{H188A}-BirA.flag, pSTV2.flag.BirA-KDM4A-ΔTT and pSTV2.KDM4A-ΔTT-BirA.flag.

Tableau 2. – Primers used in restriction cloning. Without (w/o); with (w/).

PRIMER NAME	***PRIMER SEQUENCE (5' TO 3')***
KDM4A-NOTI w/o start codon Forward	AAATATGCGGCCGCCGCTTCTGAGTCTGAAACTCTGAATCCC
KDM4A-ASCI w/ stop codon Reverse	TTGGCGCGCCCCTACTCCATGATGGCCCGGTATAGTG
KDM4A-NOTI w/ start codon Forward	AAATATGCGGCCGCCATGGCTTCTGAGTCTGAAC
KDM4A-ASCI w/o stop codon Reverse	TTGGCGCGCCCCTCCATGATGGCCCGG
KDM4A-ΔTT F3034	AAGAGAGTCAAATCTAGACTGTCAGTAGC
KDM4A-ΔTT R2688	CAAGGCCCCCTTGGCAC
KDM4A_seq. @ 870	TTTTGCTACCCGTCGGTGGATT
KDM4A_seq. @ 1606	CAAGGGCAAACGGGAGTTCTCA
KDM4A_seq.@ 2296	TGTTCAGCCAATGCCCTAGAGG
M13F	CAGGAAACAGCTATGAC
M13R	CAGGAAACAGCTATGAC
LNCX-FOR	AGCTCGTTTAGTGAACCGTCAGATC
WPRE-REV	CATAGCGTAAAAGGAGCAACA

2.3 Generation of cell lines

2.3.1 Transfection and viral production for BioID2 assay

Lentiviral production was carried out in HEK293T cells (ATCC). Before transfection, approximately 3.5 million cells were plated in a 100mm dish, covered 10mL of DMEM media (MT10017CV, Fisher Scientific) with 10% FBS (Hyclone) ; 1% Penicillin & Streptomycin (30-002-CI, Corning VWR), and incubated overnight in a 37˚C incubator with 5% CO_2. The next morning, a 60-70% confluent plate of HEK293T cells were transfected with 6µg of lentiviral plasmid DNA, 3.75µg of pSPAX.2 plasmid DNA and 1.25µg of pMD2.G plasmid DNA. The transfection reagent used is Lipofectamine 2000 (2.5 µl x µg DNA). The 11µg of DNA and lipofectamine (Invitrogen) were mixed each mixed in 500µL of OPTI MEM (11058021, Life technologies) separately, then were combined and incubated at room temperature for 5 min. In the meantime, the media of each HEK293T plate was changed and replaced with 9mL of 10%FBS, 1%pen/strep-DMEM media. The transfection mixture is then added to the appropriate HEK293T plate, which was then incubated overnight at 37˚C with 5% CO_2. Media was changed the day after into the appropriate media for the destination cell line; 10%FBS, 1%pen/strep-DMEM media (HeLa). The day after, the supernatant was collected and filtered through a 0.45µm filter unit. The collected virus was stored at -80˚C.

2.3.2 Cell line infection with lentiviral plasmid

HeLa cells (ATCC) were infected firstly with rtTA lentivirus then with the pSTV2 lentivirus. The rtTA lentiviral infection went as follows. Hela cells well plated at 40% confluency in a 100mm dish and infected with 0.5 to 1ml of rtTA the day after. 6µg/mL of polybrene was used to facilitate infection. The next the media was change and the cells were allowed to recover for 48 hours. After the recovery period, the cells were incubated in media containing 10µg/ml of blasticidin and non-infected cells we used as killing control. 5 days after the addition of the selection marker, rtTA+ Hela cells were collected, split and frozen when confluent in media containing 20%FBS (hyclone) and 10%DMSO (D4540-500ML, Sigma-Aldrich). The pSTV2 infections occurred in a similar way, however, due to the absence of a selection marker, varying volumes of the lentiviruses were added to obtain a similar level of expression. Furthermore, the

350,000 cells/60mm plate were infected with the viral volumes, 5μL of pSTV2.flag.BirA.EGFP, 10μL of pSTV2.flag.BirA.EGFP-NLS, 300μL of pSTV2.flag.BirA-KDM4A, 2600μL pSTV2.KDM4A-BirA.flag, 500μL of pSTV2.flag.BirA-KDM4A^{H188A}, 2600μL pSTV2.KDM4A^{H188A}-BirA.flag, 500μL pSTV2.flag.BirA-KDM4A-ΔTT and 2600μL pSTV2.KDM4A-ΔTT-BirA.flag. The total volume was 4mL. Cells were counted using DeNovix celldrop FL.

2.3.3 Lentiviral plasmid transduction

Lentiviral transduction in both cells lines differed slightly due to the nature of cells, adherent versus in suspension. With regards to the HeLa cell lines, the cells were plate in 150mm dishes at a 70% confluency and were induced with 0.05 - 0.5μg/mL of DOX and in a final volume of 20mL 10%FBS, 1%pen/strep-DMEM media containing 50nM of biotin. After a 24 hour incubation at 37˚C with 5% CO_2, the cells were washed 2x with cold 1XPBS (311-010-CL, Wisent) and collected in 15mL tubes. Cells were then flash frozen on dry ice and stored at -80˚C.

2.4 Visualization of expression

2.4.1 Western blot

Firstly, samples were prepared for BCA protein quantification assay. The cell pellet was resuspended in TX-100 lysis buffer (10mM Tris pH7.4, 0.5% Triton, 120mM NaCl, and protease and phosphatase inhibitors). The cells were sonicated 3x for 10sec at 30% amplitude. Samples were incubated on ice for 30 seconds in between sonications. The protein concentrations were determined through BCA assay and measured by Tecan Infinite® 200 PRO (Tecan Trading AG). Proteins were then denatured in 1XSDS sample buffer (SDS003,1, BioShop) and 10μg were fractioned onto 8% SDS-polyacrylamide gels. The proteins were transferred onto PVDF membrane, which was previously activated with methanol. The transfer occurred at 4˚C for 1 hour and 30 minutes at 100 volts (350mA) or 16 hours at 30 volts (90mA). Blocking was performed for 30 minutes at room temperature with 5% skim milk powder in TBST buffer (50 mM Tris-Cl, pH 7.5, 150 mM NaCl, 0.1% Tween 20). The membrane was washed 3x with 1X TBST buffer. The primary antibodies were diluted with antibody dilution buffer (2% BSA, 2.5% NaCl, 10mM Tris pH 7.4, 0.01% Sodium Azide) and incubated with the membrane overnight in shaking

condition at 4˚C. The following day, the membrane was washed 3x with 1X TBST and incubated with the secondary antibodies, which were diluted in 5% skim milk or 1.5% BSA depending on their reactivity with milk. The membrane was exposed with ECL reagents (PerkinElmer, Inc.) and visualized using Azure c600 (Azure Biosystems Inc.).

2.4.2 Immunofluorescence

0.1-0.15 million cells were plated in 6 well plates containing glass slides. Cultivate cells for 24 hours or until confluency is 70%. The cells were fixed with 4% paraformaldehyde (sc-281692, Santa Cruz) for 15 minutes, washed at least 3 times with 1XPBS. The cells were then permeabilized on ice for 5 minutes with 1xPBS, 3%BSA (ALB001.250, Bioshop), 0.2%Triton X-100 (ThermoFisher). This allows the antibodies to cross the cell membrane. Next, cells were blocked with 1XPBS, 3%BSA at room temperature for 10 minutes. The blocking step was repeated 3 times in total. Primary antibodies were diluted in the blocking buffer and were incubated with the cells for a period of 2 hours. To prevent the antibody evaporation, the cover glasses were each covered with parafilm and the plates were covered with damp paper towels. The cells were blocked as earlier and secondary antibodies were incubated with the cells in the dark, at room temperature for 1 hour. The cells were then washed twice with 1XPBS, 10 minutes incubation at room temperature in 1XPBS followed every wash. The cells were then stained for 10 minutes at room temperature with 4’,6’-diamidino-2-phenylindole (DAPI). The cells underwent a final wash with 1XPBS and were incubated at room temperature for another 10 minutes. Finally, one drop of mounting media was added to the slide. A cover glass was mounted onto the cells using mounting media (9990402, Fisher Scientific) and the IF slides were stored at room temperature overnight, sealed with nail polish and stored long-term in the dark at 4˚C. The images were developed using BX53 Olympus Fluorescence Upright Microscope.

Tableau 3. – List of antibodies used in this study.

ANTIBODIES	***SOURCE***	***Catalogue Number***	***WB DILUTION***	***IF DILUTION***	***SIZE (kDA)***	***BIOLOGICAL SOURCE***
Flag M2	Millipore Sigma	F3165	1:5000	1:400	50, 100, 150	Mouse
JMJD2A	Neuromab	75-189	1:1000	*NA*	100, 150	Mouse
GAPDH	SantaCruz	SC47724	1:400	*NA*	37	Rabbit
TUBULIN	Sigma	T5168	1:1000	*NA*	50	Mouse
HA	Sigma	H3663	1:1000	*NA*	35, 100	Mouse
Streptavidin-HRP conjugate	Invitrogen	19534	1:5000	*NA*	*NA*	*NA*
FBXO22	Proteintech	13606-1-AP	1:500	*NA*	45	Rabbit
ARID2	Cell Signaling	78779	1:500	*NA*	220	Rabbit
Histone H3K9me3 antibody (pAb)	Active Motif	39161	*NA*	1:400	*NA*	Rabbit
Streptavidin, Alexa Fluor™ 568 conjugate	Invitrogen	S11226	*NA*	1:200	*NA*	*NA*
Goat anti-mouse A488	Invitrogen	A11029	*NA*	1:1000	*NA*	Goat
Goat anti-rabbit A594	Invitrogen	A11012	*NA*	1:1000	*NA*	Goat
Anti-mouse IgG, HRP-linked	New England biolabs	7076S	1:3000	*NA*	*NA*	Horse
Anti-rabbit IgG, HRP-linked	New England biolabs	7074S	1:3000	*NA*	*NA*	Goat

2.5 BioID screening

The induced samples were processed by the Network Biology Collaborative Center at the Lunenfeld-Tanenbaum Research Institute, as previously described.(43) Briefly, after 24 hours induction, the samples were washed twice with cold PBS and collected into 10mL conical tubes. To pellet the cells, the samples were spun for 5 min at 450*g*. The pellet was resuspended with 1.5mL of ModRIPA buffer (50mM Tris.Cl pH7.5, 150mM NaCl, 0.5mM EDTA, 1mM EGTA, 1mM $MgCl_2$, 1% NP40, 0.1% SDS, 0.4% NaDOC, and protease and phosphatase inhibitors). The cells were sonicated 3x 30% amplitude for 5sec. TurboNuclease was added to diminish viscosity and the lysate was incubated at 4˚C for 15min, rocking. The SDS solution was adjusted to 0.4% and the lysate was spun for 15min at 15000*g*. For every samples, 25μL of streptavidin beads were used and the beads were washed once with RIPA buffer (50mM Tris.Cl pH 7.5, 150mM NaCl, 1mM EDTA, 1% NP40, 0.1% SDS, and 0.4% NaDOC). The beads were resuspended in 3:1 buffer to bead ratio and 75μL of slurry was added to the lysate supernatant.

The bead-supernatant mixture was incubated at 4˚C shaking for 3 hours. Following this incubation, the beads were spun down at 400*g* for 30 sec. The supernatant was discarded and beads were transferred into a new tube and resuspended in 500μL of RIPA buffer. The beads were then washed 1x with 2% SDS-Wash buffer (25mM Tris pH 7.5 and 2% SDS), 2x with RIPA buffer, 1x with TNTE-Wash buffer (50mM Tris 150mM NaCl, 1mM EDTA, and 0.1% NP40), and 3x with ABC (50mM Ammonium Bicarbonate).

After the washes, 50μL of ABC and 5μL of Trypsin (200ng/μL) were added and the bead slurry was incubated overnight at 37˚C. The next day, an additional 2.5μL of Trypsin (200ng/μL) was added and the samples were incubated for an additional 3 hours at 37˚C. The supernatant was then transferred into a new tube and the beads were washed with 2x with HPLC H_2O, which were polled with the supernatant leaving the beads behind. The supernatant was then spun at 10,000 rpm for 2 min to ensure that all beads were pelleted and the supernatant was transferred into a new tube. 50% Formic Acid was added, samples were dried using speed vacuum for 2-3 hours and resuspended in 5% Formic Acid. The samples were then analyzed with the 5600 TripleTOF system with an Eksigent Ultra nano-HPLC.

2.6 Streptavidin pulldown validation

The streptavidin pulldown was carried in similar fashion as the sample preparation for BioID screening, however, the samples were quantified using BCA method and 2mg/mL of lysate was used for the pulldown. In addition, after the TNTE wash, samples were eluted in 1xSDS PAGE buffer by incubating at 100˚C for 5 min.

Chapter 3 – Results

3.1 Generation BioID-inducible plasmids

In order to carry out the BioID assay, we firstly need to verify that the inducible BioID plasmids BirA-GFP, BirA-GFPNLS, BirA-KDM4A, KDM4A-BirA, BirA-KDM4A^{H188A}, BirA-KDM4A$^{\Delta TT}$, and KDM4A$^{\Delta TT}$-BirA are expressed. We did this using western blot assay. We expect that the BirA fused proteins will be expressed and the biotinylation pattern would increase upon induction. In addition, we verified the localization and functionality of KDM4A through IF. We expect that KDM4A and KDM4A$^{\Delta TT}$ would be expressed mostly in the nucleus and be able to demethylate H3K9me3. We expect KDM4A^{H188A} to also be expressed in the nucleus, but being the catalytic mutant, we do not expect it to demethylate H3K9me3. We also do not expect GFP and GFPNLS to demethylate H3K9me3. We expect GFP to be expressed in the cytoplasm and the nucleus, but we expect GFPNLS to only be expressed in the nucleus.

Following the instructions of Samavarchi-Tehrani *et al.* (2018), pSTV2 constructs were induced in HeLa cells using initially 0.5μg/mL of DOX. However, the expression of the control proteins, BirAGFP and BirAGFPNLS exceeded the expression of the proteins of interest. As a consequence, these plasmids were induced with 0.05μg/mL of DOX. Although to ensure that the hits that we generate with the BioID assay are significant, we have also analysed samples of the control cell lines induced with 0.5μg/mL of DOX.

In Figure 5, we compare the expression pattern of the different BioID constructs as well their biotinylation pattern. The induction pattern is portrayed in Figure 5A, which compares non-induced to induced lysates of the generated cell lines. We were not able to detect the expression of KDM4A-BirA and KDM4A$^{\Delta TT}$-BirA in the FLAG blot. We suspect that the FLAG tag, which is located at the C-term of BirA, is somehow masked. However, these samples were detected in the KDM4A blot. With regards to the expression pattern, BirA-KDM4A is more expressed than KDM4A-BirA and KDM4A$^{\Delta TT}$-BirA, yet slightly more expressed than BirA-KDM4A^{H188A} and BirA-KDM4A$^{\Delta TT}$ (Figure 5A). This pattern can also be observed through the

biotinylation pattern, represented here in Figure 5B. Evidently, there is an increase in biotinylation by induced cells versus non-induced cells verifying the functionality of BirA.

In Figure 6, we observed the induction and biotinylation patterns were visualized through IF. The induction pattern of the BirA fused proteins was most visible at the nuclear levels except for GFP, which seems to be expressed at the cytoplasmic level as well. The biotinylation pattern coincided with the expression pattern. In other words, there is evident biotinylation in BirA fused protein expressing cells which is present in the same compartment as the expression pattern. Consequently, we have provided additional proof that the BirA fused proteins are expressed and that BirA is functional.

After we confirmed the expression of the BirA fused proteins and the functionality of BirA through WB (Figure 5) and IF (Figure 6), we set out to confirm the functionality of KDM4A in the generated cell lines. Since KDM4A is most known to demethylate H3K9me3, we showed that cells overexpressing KDM4A will have a decrease in H3K9me3, which are pinpointed by white arrows, while non infected cells had higher levels of H3K9me3, which are pinpointed by yellow arrows (Figure 7). The catalytic mutant, KDM4A-H118A is unable to demethylate H3K9me3. The TT mutant retained its catalytic activity and was able to bind and demethylate H3K9me3, showing that successful demethylation of H3K9me3 is somewhat independent of the TT domain. As expected, the demethylation pattern is not observed in the control cell lines expressing BirAGFP and BirAGFPNLS.

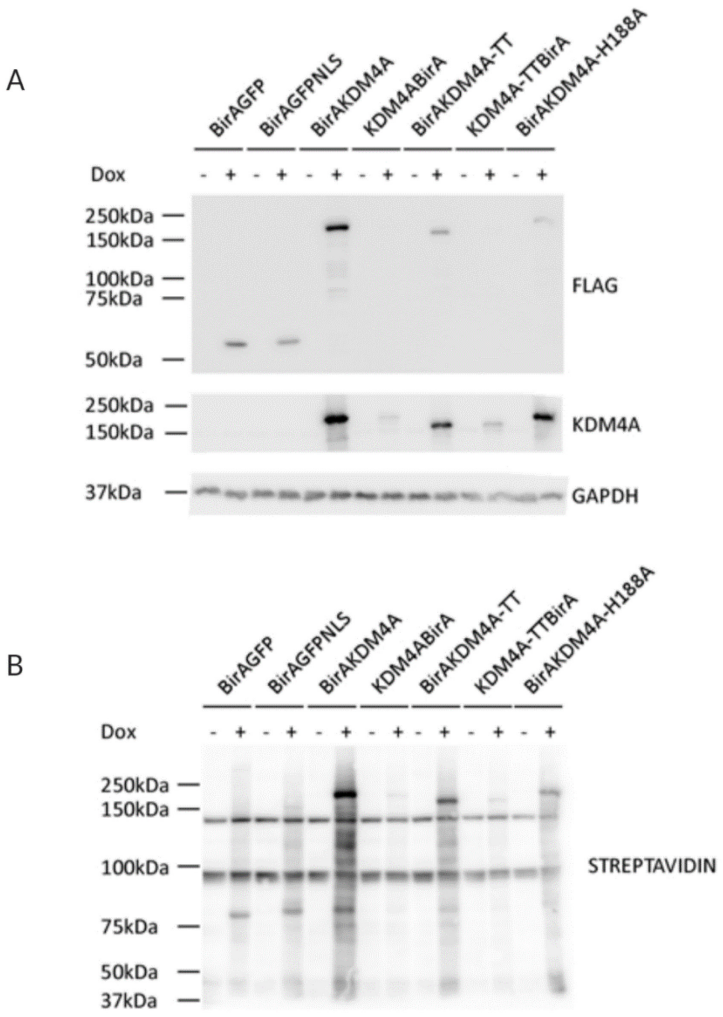

Figure 5. – Generation of BirA-tagged KDM4A-inducible HeLa cell lines. A) Expression levels of the different BioID constructs used in this study. B) Biotinylation pattern across the controls and the different experimental constructs used in this study. Created with BioRender.com

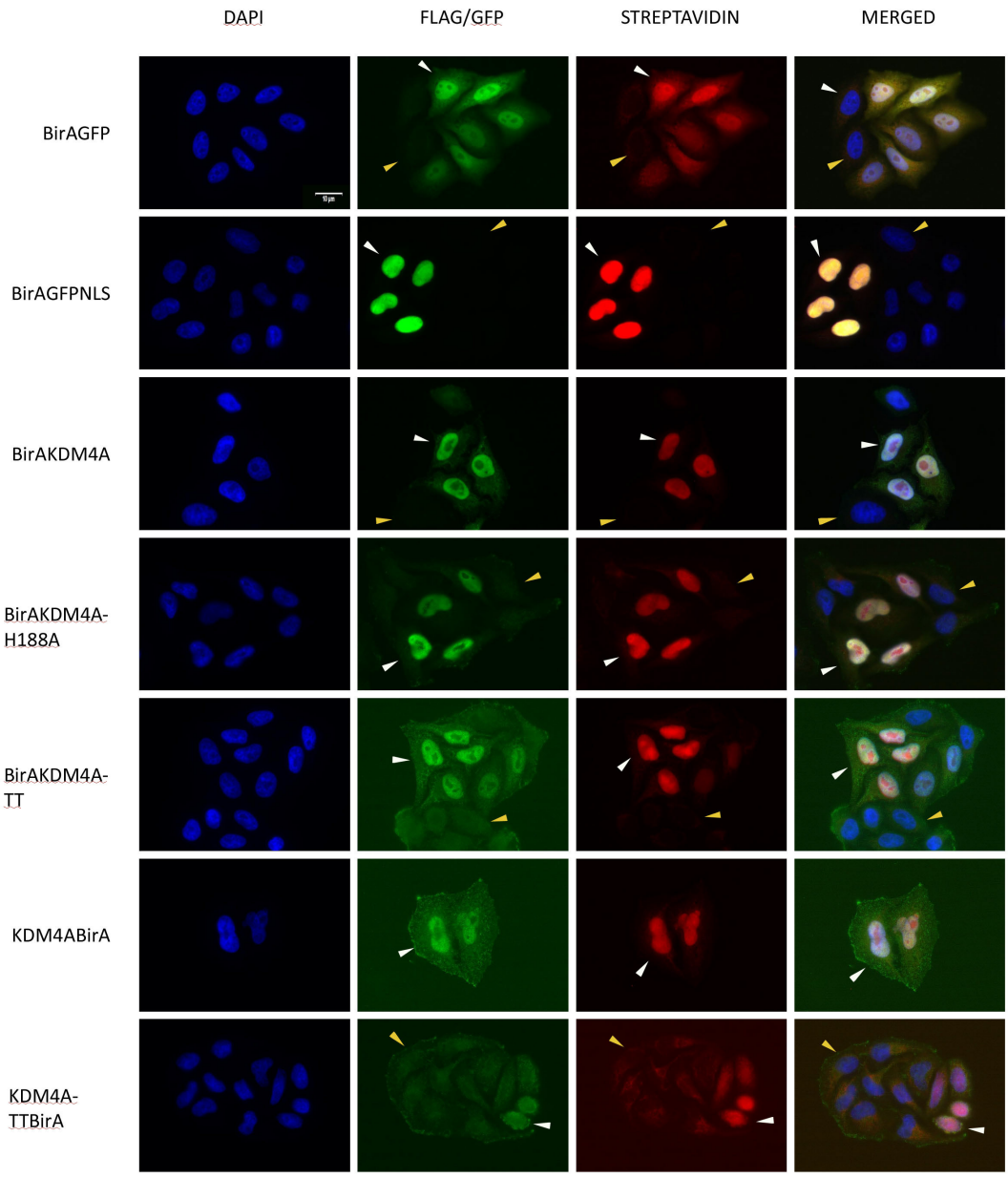

Figure 6. – Validation of expression and biotinylation patterns of generated cell lines. The columns depict the staining pattern, while the rows represent the different cell lines. Induction pattern, expressed in green, seems to be prevalent at the nuclear level, shown through DAPI staining. In this case, induced cells are considered as infected cells and non-infected cells do not harbor the BirA fused proteins. Biotinylation pattern, expressed in red, seems to overlap with the induction pattern. There is a clear difference in the biotinylation pattern between infected (white arrow) versus non-infected (yellow arrow) cells.

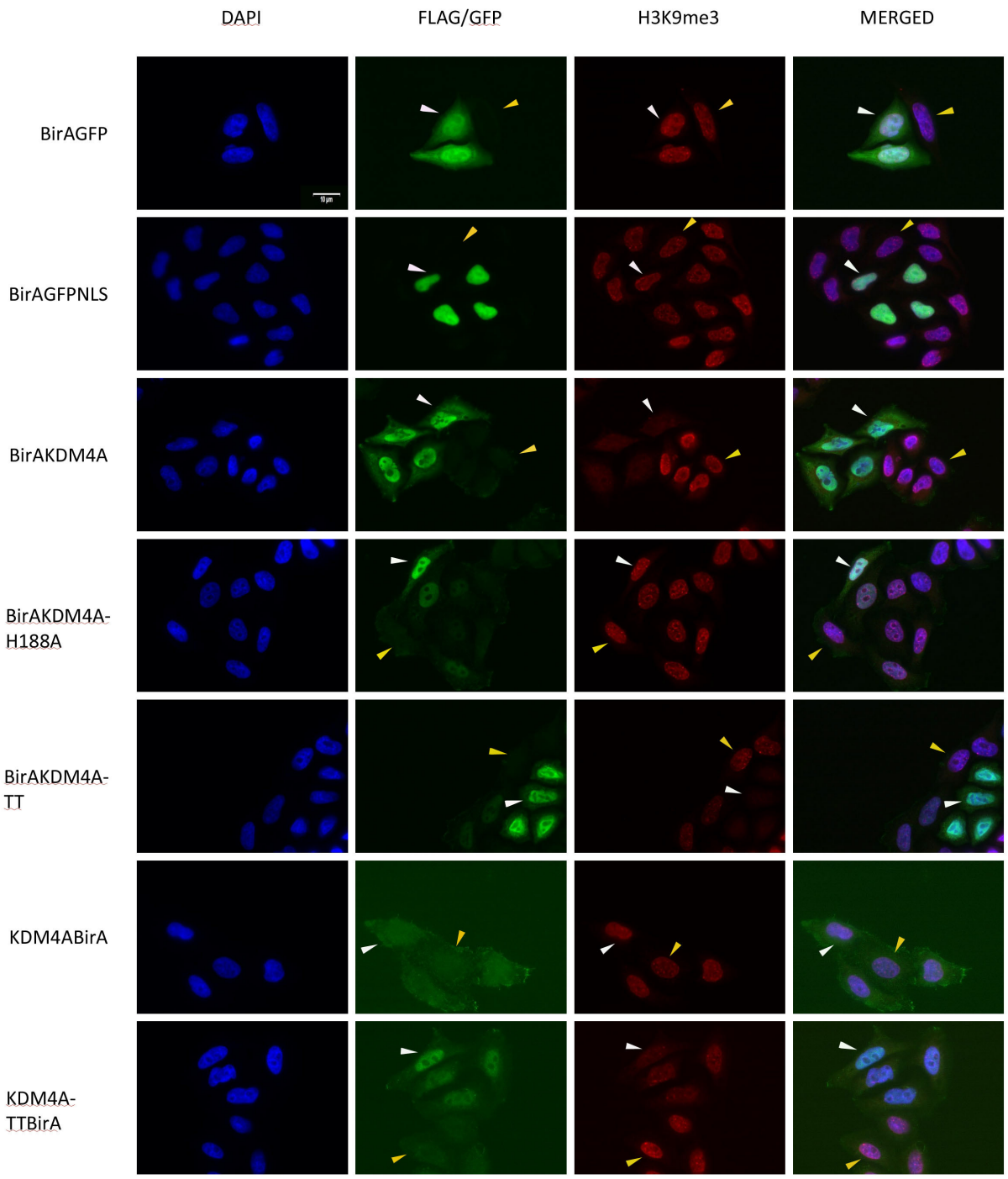

Figure 7. – Validation of the catalytic activity of KDM4A. The columns depict the staining pattern, while the rows represent the different cell lines. The induction pattern, represented here in green, is mostly at the nuclear level. The H3K9me3 pattern, represented here in red, depicts foci of H3K9me3.

3.2 Mass spectrometry results and analysis

The potentially interacting partners of KDM4A were selected for their biotinylation pattern through streptavidin pulldown and they were identified through MS. The results were analysed using SAINTexpress statistical software. These were carried out by the Network Biology Collaborative Center at the Lunenfeld-Tanenbaum Research Institute. We expect to isolate proteins that are significantly interacting with KDM4A and to further identify the interactions that are dependent on the catalytic activity of KDM4A and/or its TT domain by comparing the list of interactants of each BirA fused protein sample.

Furthermore, the interacting proteins that were considered as significant had an FDR equal to or below 0.05. As mentioned earlier, the control cell lines were induced with 0.5 and 0.05μg/mL of DOX. Furthermore, the statistical analysis included with induction patterns of the control cell lines. However, with the overexpressed BirAGFPNLS sample used as control, there were only 13 KDM4A significant interacts, which will from now on be referred to as hits. Among these hits were ARID2, BRD7 and SMARCA2, which are members of the pBAF complex (52,53). Other interesting hits were FBXO22, a protein known to interact with KDM4A (32,69), and SCL2A1, a glucose transporter corelated with bad cancer prognosis (62,104).

Consequently, we set BirAGFPNLS as a bait instead of control and the resulting list of KDM4A interacting proteins became extensive with 186 hits. We triaged this list by eliminating proteins that interact with BirAGFPNLS with an FDR equal to or below 0.05, which totaled 142 hits. The remaining hits underwent another triage which eliminated BirAGFPNLS interacting proteins equal to or below 0.1 FDR, which removed 3 hits from the list. The resulting list consisted of 41 proteins, represented here in Table 4 and Figure 8, that seem to be interacting significantly with KDM4A.

This list comprised of almost all the members of the pBAF complex, except for PBRM1. It also included some DNA damage proteins such as BRCA2, XRCC5, and XRCC6. Notably, there were several RNA binding proteins such as ELAVL1, RBM5, MTREX/SKIV2L2, FUS, and PHF5A. Some of these interactions are lost depending on the catalytic activity and TT domain of KDM4A. As an example, the interaction with FBXO22 is lost with the catalytic down mutant while the

interaction with BRCA2 is lost with the TT mutant. These lost interactions can be observed clearly in Figure 8 and are represented in Table 4 by the high or nonsignificant (NS) FDR.

Using © STRING CONSORTIUM 2020, a functional protein association map of the KDM4A significantly interacting proteins was generated (Figure 9). These proteins were also organized according to their biological function in Table 5. Furthermore, most of these proteins are transcription factors, which is something we excepted since previously characterized KDM4A protein interactions are mostly transcription factors (Table 1). KDM4A seems to also interact with chromatin remodelers, DNA damage response proteins and H3K36 demethylases (Table 5). Additionally, KDM4A seems to be interacting with RNA splicing proteins and organic transmembrane transporters, which are to our knowledge novelties.

Tableau 4. – KDM4A interacting proteins generated from BioID analysis. The peptide recovered replicates are presented for BirA-EGFP and BirA-EGFPNLS. A false discovery rate (FDR) was presented for BirA-EGFPNLS and the experimental samples. NS; non-significant.

Proteins	Protein full name	Protein ID	BirA-EGFP recovered peptides	BirA-EGFPNLS recovered peptides	BirA-EGFPNLS FDR	BirA-KDM4A FDR	KDM4A-BirA FDR	BirA-KDM4A ΔTT FDR	KDM4A ΔTT-BirA FDR	BirA-KDM4^{H188A} FDR
ARID2	AT-rich interactive domain-containing protein	NP_689854.2	0|0|0	4|0|0	0.21	0.01	0.5	0	0	0
ZNF217	Zinc finger protein 217	NP_006517.1	0|0|0	0|0|0	NS	0	NS	0.11	NS	0
FBXO22	F-Box Protein 22	NP_036302.1	0|0|2	0|0|0	NS	0.01	0.36	0.02	0.36	NS
BRCA2	BRCA2 DNA Repair Associated	NP_000050.2	0|0|0	5|0|0	NS	0.01	NS	0.16	NS	0
SMARCA2	SWI/SNF Related, Matrix Associated, Actin Dependent Regulator of Chromatin, Subfamily A, Member 2	NP_003061.3	0|0|0	0|0|0	NS	0	NS	NS	NS	NS
SMARCC2	SWI/SNF Related, Matrix Associated, Actin Dependent	NP_001123892.1	0|0|0	6|0|0	0.16	0	NS	0.18	0	0.28

	Regulator of Chromatin Subfamily C Member 2									
XRCC6	X-Ray Repair Cross Complementing 6	NP_001460.1	0|0|0	16|0|0	0.11	0	NS	0.14	NS	0
ELAVL1	ELAV Like RNA Binding Protein 1	NP_001410.2	0|0|6	6|2|3	0.34	0.04	0.34	0.39	0.38	0.37
CACYBP	Calcyclin Binding Protein	NP_001007215.1	0|0|0	0|0|0	NS	0	NS	0	NS	0
RBM5	RNA Binding Motif Protein 5	NP_005769.1	0|0|0	10|0|0	0.12	0	NS	0.24	NS	0.15
PHF8	PHD Finger Protein 8	NP_001171825.1	0|0|0	6|0|0	0.16	0	NA	0.16	NS	0
NUP107	Nucleoporin 107	NP_065134.1	0|0|0	8|0|0	0.14	0	NS	NS	NS	0
ZNF335	Zinc Finger Protein 335	NP_071378.1	0|0|0	2|0|0	0.28	0	NS	NS	NS	0.24
BRD7	Bromodomain Containing 7	NP_001167455.1	0|0|0	0|0|0	NS	0	NS	0.14	0.18	0
SLC16A3	Solute Carrier Family 16 Member 3	NP_001035887.1	0|0|0	2|0|0	0.28	0	0.24	0.24	NS	0.16
PSMC1	Proteasome 26S Subunit, ATPase 1	NP_002793.2	0|0|0	5|0|0	0.18	0	NS	0	NS	0
MFAP1	Microfibril Associated Protein 1	NP_005917.2	0|0|0	6|0|0	0.16	0	NS	0.24	0.24	0
AP3M1	Adaptor Related Protein Complex 3 Subunit Mu 1	NP_036227.1	0|0|0	0|0|0	NS	0	NS	0.16	NS	0
MTREX	Mtr4 Exosome RNA Helicase	NP_056175.3	0|0|0	9|0|0	0.13	0	NS	0	NS	0
SLC16A1	Solute Carrier Family 16 Member 1	NP_001159968.1	0|0|0	3|0|0	0.24	0	0.24	0.24	0.28	0
KDM2A	Lysine Demethylase 2A	NP_001243334.1	0|0|0	4|0|0	0.21	0	NS	0.28	NS	0
ING3	Inhibitor of Growth Family Member 3	NP_061944.2	0|0|0	4|0|0	0.21	0	NS	0.24	NS	0.21
PSMD1	Proteasome 26S Subunit, Non-ATPase 1	NP_001177966.1	2|0|0	4|0|0	0.34	0.01	NS	0.36	NS	0.01
SMARCE1	SWI/SNF Related, Matrix Associated, Actin Dependent Regulator of Chromatin,	NP_003070.3	0|0|0	3|0|0	0.24	0	NS	0	0.28	0.28

	Subfamily E, Member 1									
FUS	FUS RNA Binding Protein	NP_001164105.1	0|0|0	5|0|0	0.18	0	NS	0.24	0.28	0
SIX5	SIX Homeobox 5	NP_787071.2	0|0|0	5|0|0	0.18	0	NS	NS	NS	0
SUB1	SUB1 Regulator of Transcription	NP_006704.3	0|0|0	7|0|0	0.15	0	NS	0	NS	0
SRCAP	Snf2 Related CREBBP Activator Protein	NP_006653.2	0|0|0	4|0|0	0.21	0	NS	0.28	NS	NS
XRCC5	X-Ray Repair Cross Complementing 5	NP_066964.1	0|0|0	4|0|0	0.21	0	NS	NS	NS	0.28
CDC37	Cell Division Cycle 37, HSP90 Cochaperone	NP_008996.1	0|0|0	0|0|0	NS	0	0.5	0.18	NS	0.24
SLC2A1	Solute Carrier Family 2 Member 1	NP_006507.2	0|0|0	0|0|0	NS	0	NS	0.24	NS	0.28
CENPE	Centromere Protein E	NP_001804.2	0|0|0	0|3|0	0.24	0	0.36	NS	NS	NS
PHF5A	PHD Finger Protein 5A	NP_116147.1	0|0|0	0|0|0	NS	0.21	NS	NS	NS	NS
POLDIP3	DNA Polymerase Delta Interacting Protein 3	NP_115687.2	0|0|0	7|0|0	0.15	0	NS	NS	NS	0.28
CWF19L1	CWF19 Like Cell Cycle Control Factor 1	NP_060764.3	0|0|0	0|0|0	NS	0	NS	0.21	NS	0.24
NUP160	Nucleoporin 160	NP_056046.1	0|0|0	0|0|0	NS	0	NS	0.28	NS	0.28
PSMD2	Proteasome 26S Subunit, Non-ATPase 2	NP_002799.3	0|0|0	0|0|0	NS	0	0.34	0.18	NS	NS
ZNF207	Zinc Finger Protein 207	NP_001027464.1	0|0|0	4|0|0	0.21	0.01	NS	NS	NS	0.24
BTF3	Basic Transcription Factor 3	NP_001032726.1	0|0|0	2|0|0	0.28	0.01	NS	NS	NS	0.28

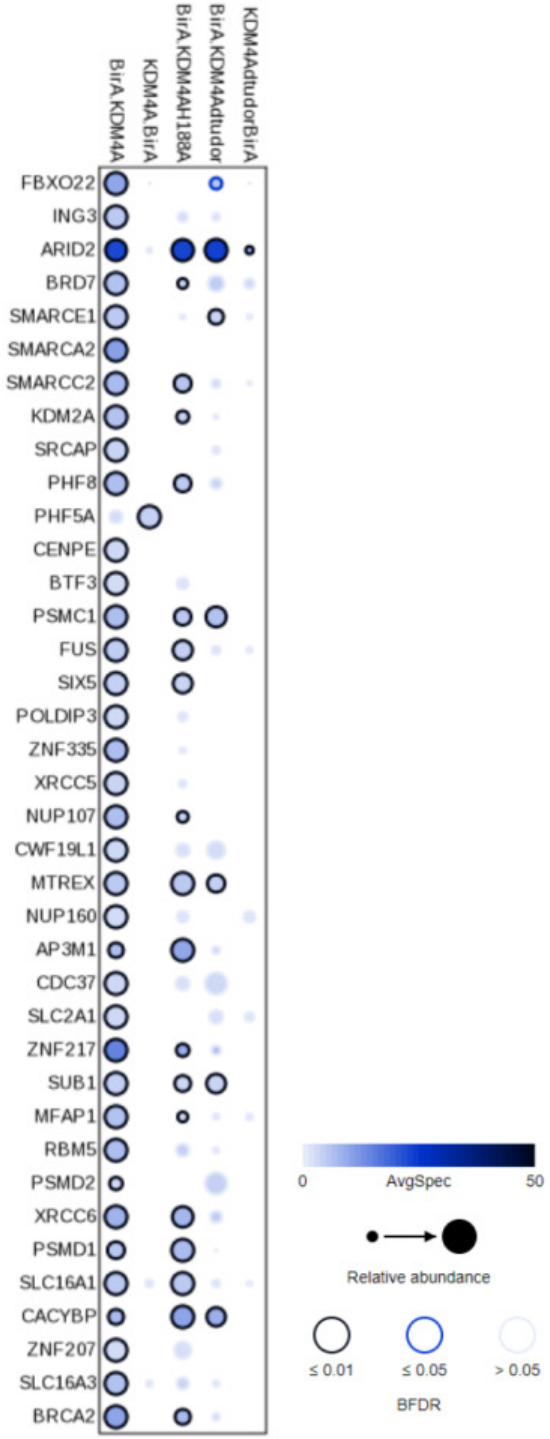

Figure 8. – Dot plot portraying the protein KDM4A interaction network. The color represents the average spectrum while the relative abundance is represented by the size of the dot. The FDR is represented by the outline of the dot. Created with BioRender.com

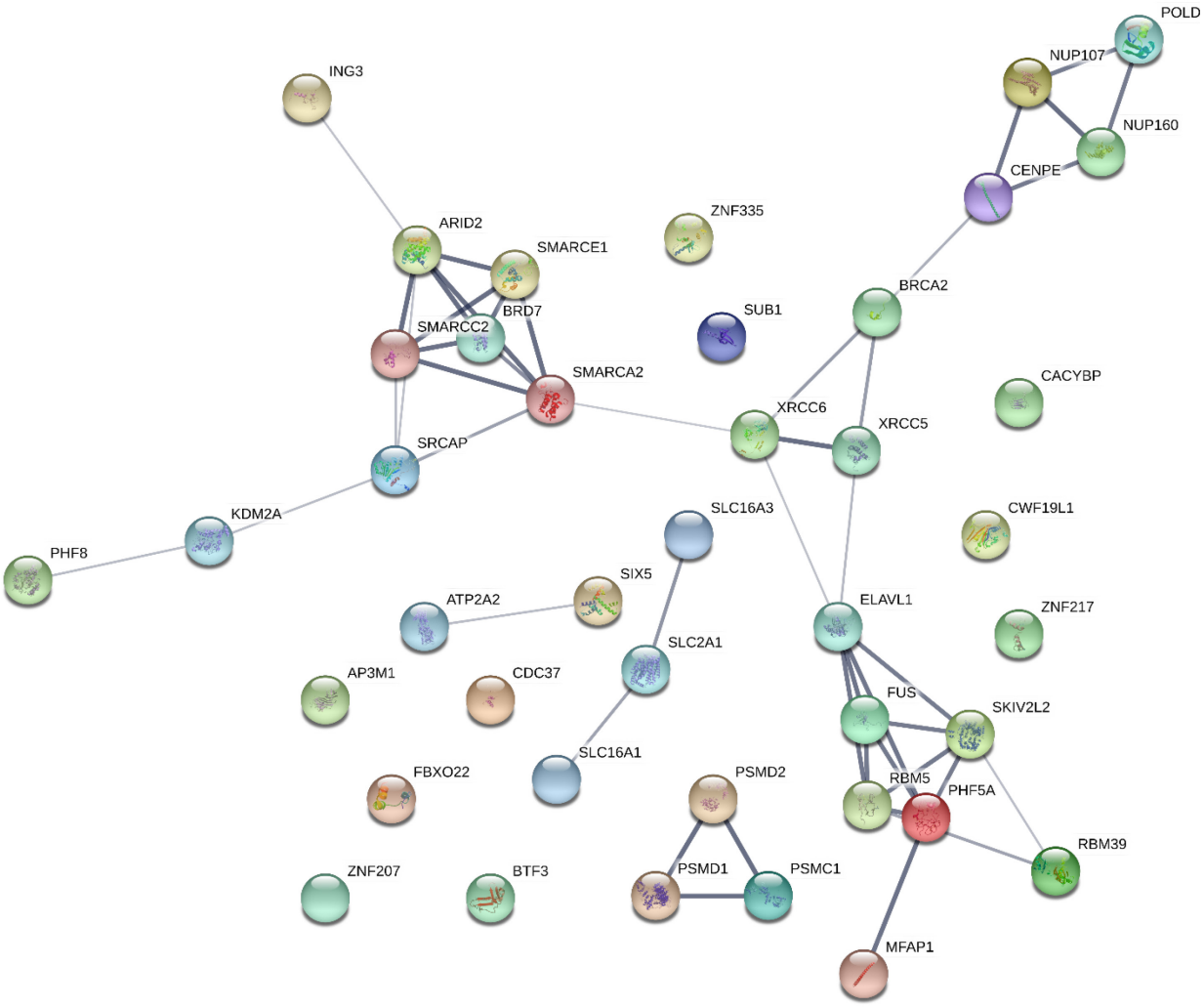

Figure 9. – Functional protein association map of KDM4A interacting proteins obtained from © STRING CONSORTIUM 2020. The line thickness indicated the interaction confidence. The threshold confidence was set to medium confidence (0.4).

Tableau 5. – List of proteins interacting significantly with KDM4A organized by their biological function adapted from © STRING CONSORTIUM 2020.

Biological function	**Proteins significantly interacting with KDM4A**
DNA-binding transcription factor	ARID2, KDM2A, PHF5A, SIX5, SMARCC2, SMARCE1, SUB1, ZNF207, ZNF217, ZNF335
Histone modification	BRCA2, ING3, KDM2A, PHF8, SRCAP, ZNF335
Transcription coactivator	BRD7, FUS, SMARCA2, SMARCC2, SMARCE1, SRCAP, SUB1
RNA splicing	ELAVL1, FUS, PHF5A, RBM39, RBM5, MFAP1
Histone H3-K36 demethylation	KDM2A, PHF8
Organic anion transmembrane transporter	SLC16A1, SLC16A3, SLC2A1
Nucleocytoplasmic transport	FBXO22, NUP107, NUP160, POLDIP3
Proteasome	PSMC1, PSMD1, PSMD2
DNA recombination	BRCA2, XRCC5, XRCC6
S100 protein binding	ATP2A2, CACYBP

3.3 Validation of BioID assay results

To validate the BioID assay results, we carried out streptavidin pull down on the lysates of the induced BioID cell lines, shown here in Figure 10. Firstly, we verified that KDM4A, KDM4A-ΔTT, KDM4A^{H188A} and the control proteins, GFP and GFPNLS, were pulled down, shown here in the FLAG and KDM4A blots of Figure 10. The control proteins, BirA.KDM4A, BirA.KDM4A-ΔTT and BirA.KDM4A^{H188A} were pulled down. However, KDM4A-ΔTT.BirA was barely present and KDM4A.BirA was not present in the pulled-down. This could be due to their low expression, represented here in the INPUT KDM4A blot (Figure 10).

Then we verified two of the top three interacting proteins (Table 4) that have the most recovered peptides, ARID2 and FBXO22. According to the SAINTexpress analysis, ARID2 seems to be within the labeling radius of BirAKDM4A, BirAKDM4A-ΔTT and BirAKDM4A^{H188A}. We expected ARID2 to be pulled down with BirAKDM4A, BirAKDM4A-ΔTT and BirAKDM4A^{H188A};

however, it was only pulled down with BirAKDM4A (Figure 10-ARID2 blot). In contrast with ARID2, FBXO22 is known to interact with KDM4A. Interestingly, according to our results, this interaction seems to be dependent on KDM4A's catalytic activity since there were no recovered peptides from either replicate (Table 4). FBXO22 was pulled down with all the constructs but most significantly with BirAKDM4A and BirAKDM4A-TT, which coincides with the results obtained from the BioID assay (Figure 10-FBXO22 blot). Finally, Tubulin, a protein that does not interact with KDM4A, was not recovered in the pull down, which in turn validates the specificity of this pull down (Figure 10-Tubilin blot).

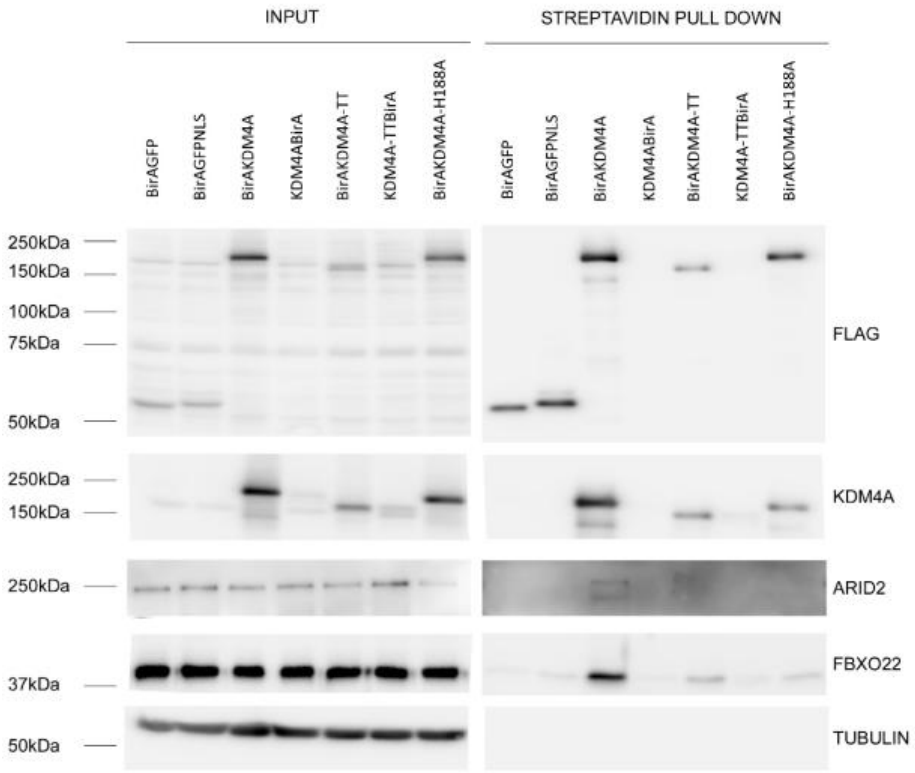

Figure 10. – Validation of BioID assay results through streptavidin pull down. BirAGFP, BirAGFPNLS, BirAKDM4A, BirAKDM4A-ΔTT, BirAKDM4A^{H188A}, and KDM4A-TTBirA were recovered. ARID2 and FBXO22 are the within the labeling radius of KDM4A. Tubulin does not interact with KDM4A.

Chapter 4 – Discussion

4.1 KDM4A interacting proteins

In this study, we sought out to identify KDM4A interacting proteins to better understand its role in carcinogenesis. We used BioID2 to be able to detect direct and indirect protein interactors of KDM4A and we decided that cervical cancer would be the optimal model since it has been recently established that KDM4A is involved in cervical cancer tumorigenesis (31-35). Furthermore, our results highlighted that KDM4A mainly interacts with transcription factors such as ARID2, SMARCC2, SMARCE1, SUB1, KDM2A, PHF5A, SIX5, ZNF207, ZNF217, ZNF335 (Table 5). Interestingly, two H3K36 demethylases KDM2A and PHF8 were also identified by BioID, which was highlighted by © STRING CONSORTIUM 2020. As an epigenetic regulator, KDM4A's main role is to regulate gene expression by demethylating H3K9me2/3 and H3K36me2/3, which can either promote or repress gene expression (7-9). Furthermore, KDM4A could competing with these demethylases.

Another process that KDM4A shares with its interacting counterparts is DSB repair via NHEJ (18). According to the results generated from the MS analysis, summarized here in Table 4, and the analysis generated from © STRING CONSORTIUM 2020, summarized in Table 5, there are 3 candidates that are assigned to this biological process: KDM2A, XRCC5, and XRCC6. BRCA2, which also seems to interact with KDM4A, plays a crucial role in DSB repair, by directly interacting with RAD51 and promoting recombination and DNA repair. However, it is mostly involved in HR rather than NHEJ (49). Furthermore, this result could that KDM4A may play a broader role in DDR than previously thought. DDR is often deregulated in cancer further bringing focus to KDM4A's integral role in tumorigenesis (16).

It was also promising to see that FBXO22 is among the possible interacting partners of KDM4A since it has been previously described (32). FBXO22 was found to target KDM4A for degradation. Interestingly, according to our results, it seems to be dependent on its catalytic activity (Table 4, Figure 8). This result is further reiterated in Figure 10, where it is evident that FBXO22 interacts with KDM4A and its TT mutant, while the amount of FBXO22 pulled down with

the catalytic down mutant KDM4A^{H188A} resembles that of the controls GFP and GFPNLS. Previously, it was found that KDM4A interacts with FBXO22 for the targeted degradation of methylated p53 by facilitating the interaction of FBXO22 to the p53 CTD domain (69). However, the expression of a catalytic mutant of KDM4A lead to the stabilization of p53 (69). Furthermore, taken together this information and our results, we can further emphasize the importance of the interaction of FBXO22 and the catalytic active KDM4A to target methylated p53 for degradation (69,70). Consequently, according to our results, this interaction could be lost with a catalytically inactive KDM4A. Moreover, this further highlights the role of KDM4A in tumorigenesis, which is aiding in the degradation of p53, a tumor suppressor (70).

Considering all these points, we can assume that the existence of novel interactions should be studied further. For instance, KDM4A seems to be interacting with multiple components of the pBAF chromatin remodeling complex, such as ARID2, BRD7, SMARCA2, SMARCC2 and SMARCE1. In Figure 11 we have validated through streptavidin pull down that ARID2 is in the biotinylation radius of BirAKDM4A and thus could be a potential interactor. According to the MS analysis this interaction is independent of KDM4A's catalytic activity and TT domain. However, this could not be replicated in the streptavidin pull down (Figure 11). One reason could be the efficiency of the antibody, which is accessed by sensitivity and specificity. ARID2 polyclonal antibody seems to be specific to ARID2, but not as sensitive. Another reason would be that the levels of KDM4A-TT pull down is not as efficient as the wildtype KDM4A pull down.

4.2 KDM4A and the pBAF complex

The Polybromo-associated BAF complex, also known as pBAF complex, is one of two chromatin remodeling complexes, the other being the BAF complex (52). These complexes are ATP-dependent and thus require ATP to remodel histones, which allows for epigenetic regulation of gene expression (52,100). The subunits of the pBAF complex are BAF200/ARID2, BAF180/PBRM1, SMARCA4/BRG1 or SMARCA2, BAF170/SMARCC2, BAF155/SMARCC1 and BAF51/SMARCE1 (52,53). According to our results, KDM4A seems to be interacting with ARID2, BRD7, SMARCA2, SMARCC2 and SMARCE1. However, ARID2 peptides seem to be increasingly isolated compared to the rest (Table 4, Figure 8). We can infer that KDM4A could be interacting

with the pBAF complex via ARID2 and this interaction is not dependent on KDM4A's catalytic activity or TT domain. However, the rest of the pBAF subunits that seem to be interacting with KDM4A are dependent on KDM4A's catalytic activity and/or TT domain. Furthermore, SMARCA2, SMARC2, and SMARCE1 seem to be dependent of both the catalytic activity and TT domain of KDM4A, while BRD7 seems to be dependent on its TT domain (Table 4, Figure 8). Consequently, KDM4A could be interacting directly and indirectly with the subunits of the pBAF complex.

ARID2 was found to be essential for the stability of the pBAF complex and could be involved in the recruitment of the PBRM1 into the complex (53). PBRM1 was previously thought to be the specificity subunit of the pBAF complex, however new evidence has shown that the pBAF complex is able to function normally in the absence of PBRM1 (53,102). Furthermore, ARID2 was found to be crucial to the functionality of the pBAF complex and in the absence of PBRM1, which occurs in some cancer types, it can form new functional pBAF complex. Although ARID2 is indispensable to the pBAF complex, both ARID2 and PBRM1 play a role in directing the complex to different genes, either through protein-protein interactions or protein-DNA interactions (53). KDM4A has previously been documented to stabilize DEPTOR to prevent its degradation (28). Furthermore, KDM4A could be influencing the stability of the pBAF complex through its interaction with ARID2 or the localization of the pBAF complex.

Several of the pBAF subunits are recurrently mutated in cancer, especially PBRM1 and ARID2 (54,55). The reason behind this is tied to the role of this complex in controlling immune system recruitment and T-cell activation through INFγ signalling (54). For instance, PBRM1 mutations are predominant (approximately 41%) in patients suffering from clear cell renal cell carcinoma, while ARID2 mutations are predominant in melanoma (55). Furthermore, it was also found that PBRM1, ARID2, and BRD7 deficient melanoma tumor cells are more sensitive to T-cell mediated toxicity since the pBAF complex seems to reduce the chromatin accessibility to INFγ-inducible genes (54). Consequently, targeting these genes would be ideal to complement immunotherapy such as PD-1 and PD-L1 blockade, since it would further sensitise the tumor to T-cell inflammatory activity (54,55).

Conversely, ARID2 has been labeled as a tumor suppressor in hepatitis C-associated hepatocellular carcinoma (56-58). ARID2 was silenced through frame-shift deletion, nonsense mutation or splice site alteration. In addition, ARID2 deletion seems to affect the expression levels of the other subunits of the pBAF complex and in consequence, affecting the presence of pBAF complex in these tumors (56). Interestingly, ARID2 seems to play a major role in the transcription of interferon-induced transmembrane protein 1 (IFITM1), which in turn promotes anti-proliferative activity through IFN induction (57). Furthermore, ARID2 gene targeting in hepatocellular carcinoma was found to promote proliferation (56-58).

4.3 KDM4A TT domain and DSB repair

According to our results, the interaction of KDM4A with the proteins involved in DDR seems to be dependent on the TT domain. As mentioned earlier, KDM4A interacts with KDM2A, XRCC5, XRCC6, and BRCA2, which are proteins that play a role in DSB repair (Table 4 and Figure 8, 10). Our results show that these interactions are lost in the absence of the TT domain. Looking back at Figure 3, KDM4A must be degraded to allow the binding of 53BP1 to H4K20me2 in order to initiate NHEJ repair pathway (18). Since KDM4A binds to H4K20me2 through its TT domain (8), these results reiterate KDM4A's role in NHEJ and further links its role to the TT domain. This was also previously described by Mallette et al. (2012), where the recruitment of 53BP1 to the site of DSBs was partially re-established in RNF8/168 deficient U2OS osteosarcoma cells infected with JMJD2AD939R, which retains the ability to bind to H4K20me2. In addition, they also found that the catalytic down mutant KDM4A^{H188A} did not re-establish 53BP1 recruitment, therefore, the role of KDM4A in DSB repair is independent of its catalytic activity but dependent on its TT domain (18).

4.4 KDM4A and mRNA splicing

As mentioned earlier, KDM4A is an epigenetic regulator that alters gene expression through its demethylation activity (5-8). Our results hint at the possibility that KDM4A may have an influence on the expression of proteins by interacting with proteins that play a role in RNA splicing such as ELAVL1/HuR, RBM5, MTREX/SKIV2L2, FUS, and PHF5A (Table 4 and Figure 8, 10). One noteworthy interactor is ELAVL1, also known as HuR, which plays a role in mRNA stability

by binding to adenylate/uridylate (AU) - and U-rich elements in the UTR or poly(A) tail of RNA (59). Over the years, ELAVL1 has been described as an oncogene and a tumor suppressor (59,103). Its oncogenicity is linked to poor prognosis, metastasis and advanced stages of cancer (59). ELAVL1 is a nuclear protein, however, since it is crucial for mRNA stability, it is transported into the cytoplasm (59,103). Furthermore, high levels of cytoplasmic ELAVL1 are recorded in several cancers such as oral, colorectal, lung, breast and ovarian cancers. Its target mRNAs are oncogenes, CDKs, apoptosis related molecules and methyltransferases (59).

Interestingly, elevated levels of cytoplasmic ELAVL1 was correlated with aggressive clinicopathologic features in uterine cervical cancer (59,60). More specifically, ELAVL1 seems to influence the expression of cyclooxygenase-2 (COX-2) mRNA (60). COX-2 is crucial for the synthesis of prostaglandins. ELVAL1 seems to stabilize COX-2 mRNA and in consequence promotes an increase in the expression of COX-2 protein, which is linked to bad prognosis (59,60). In ovarian cancer, ELAVL1 was found to be inhibited by mRNA139-3p, a tumor suppressor (61). Furthermore, KDM4A's interaction with ELAVL1 could also resemble its interaction with DEPTOR (18). In other words, KDM4A could be affecting the stability of ELAVL1. If KDM4A affects the stability of ELAVL1, then by association, it would have an effect on COX-2 protein expression.

4.5 KDM4A and organic anion transport

KDM4A seems to be interacting with three organic anion transporters: SLC16A3, SLC16A1, and SLC2A1. A recent study analyzed the prognostic value of different organic anion transporters in order to predict patient survival and deemed SLC16A3, SLC16A1 and SLC2A1 as "unfavorable" (62). SLC16A3 and SLC16A1 are monocarboxylate transporters involved in lactate, pyruvate or ketone bodies transport. These transporters contribute to the tumor environment by promoting a more alkaline pH, which is a characteristic of aggressive tumors (62,72). In melanoma, both transporters are upregulated and are associated with "unfavorable" prognosis (62). Their downregulation highlighted their involvement in glycolysis, pH and ATP production, which are all factors that are important to maintain the tumor environment. SLC2A1, also known as GLUT1, is a glucose transporter and thus contributes to the tumor cells' energy (62,104).

Interestingly, SLC16A3 seems to be overexpressed in hypoxic conditions and to play an important role in in hypoxic cancer growth (72). Hypoxic conditions are favored in most tumor cells and these tumors are characterized as being more aggressive and resistant to therapy (73). Hypoxic tumors rely on glycolysis, which generate a lot of lactate and thus affects the pH of the cell (72,73). SLC16A3 expels the lactate outside the cell thus maintaining neutral pH and preventing cell apoptosis (72). Previously, KDM4A has been described to play in promoting hypoxic conditions in cancer cells by regulating HIF-1α mRNA expression (74). In addition, HIF-1α was found to regulate the expression of SLC16A3 (72). Furthermore, there seems to be some downstream nuclear connection between SLC16A3 and KDM4A (72,73,74). By association, KDM4A could be interacting with SLC16A3 to stabilize the transporter and further promote hypoxic conditions. SLC16A3 inhibitors, such as diclofenac, are currently being investigated as therapeutics for cancer treatment (75). This magnifies the importance of further characterizing the interaction between KDM4A and SLC16A3.

4.6 Efficiency of BioID2 assay to detect protein-protein interactions

There were technical difficulties to attain equal levels of protein expression across all samples. The reason for that is if the ORF of the BAIT is long, the choice of destination vector that carries BirA is limited. In other words, our options were limited to pSTV2, designed by Samavarchi-Tehrani P et al. (2018), which does not have a reporter gene or selection marker (43). Furthermore, the expression levels can vary between the different cell lines as well as different replicates. However, averaging the interaction scores between the two replicates allows for more consistent results. Taking this into account, the BioID results seem to be consistent with KDM4A localization and function (Table 4). another disadvantage of BioID2 is the inability to distinguish between direct and indirect interactions, however it can detect transient interactions (40,41). Consequently, additional validations are required to be able to identify the type of interactions.

4.7 Perspective

Considering that KDM4A is being targeted for cancer therapy (7-9,36), the results presented in this study can be further used and verified to establish the divergent role of KDM4A in

tumorigenesis and cancer development. BioID2 seems to be a sensitive technique to detect direct and indirect protein-protein interactions, however further validation of these interactions is required (40,41).

4.7.1 Validation of KDM4A interaction with FBXO22

Further validation of the involvement of the catalytic activity of KDM4A for its interaction with FBXO22 could be done through Glutamine S-transferase (GST) pulldown. However, instead of coupling KDM4A to GST, fragments of KDM4A with or without the JMJC catalytic domain will be coupled to a GST tag. This method has been proven to be effective at identifying strong protein-protein interactions as well as domain specific interactions (50). According to our data (Table 4, Figure 8) KDM4A's interaction with FBXO22 is independent of its TT domain, consequently, we can use a fragment of KDM4A containing only the TT domain as a negative control. In other words, we would not expect FBXO22 interact with the TT domain, but to successfully interact with JMJC domain. As a positive control we will be coupling KDM4A wildtype to a GST tag. To further pinpoint the interaction site of FBXO22, we would use a fragment containing the JMJC domain with the H188A amino acid substitution. With this method we can validate and confirm the results obtained from the BioID2 assay. Finally, FBXO22 could also be tagged with HA or FLAG, which would allow us to verify if KDM4A or its mutants are co-purified with the FBXO22 pull down.

4.7.2 Validation of KDM4A interaction with ARID2 and the pBAF complex

Consequently, further validation of this interaction can be carried out with FLAG-immunoprecipitation (IP). Flag-IP consists of tagging the protein of interest, in this case KDM4A, with a FLAG tag and immunoprecipitating KDM4A. Ideally, proteins that directly interact with KDM4A will precipitate as well; however, this may pose some difficulty in isolating interactions that are not stable or strong.

One way to analyze transient or weak protein interactions is through chemical crosslinking. This method is comprised of using a chemical probe, such as N-hydroxysuccinimide (NHS)-ester-crosslinker, to create a covalent bond with the transiently interacting protein (50). The crosslinks generally target lysine side chains of the interacting proteins. Crosslinked proteins can

then be detected by SDS-PAGE and WB, where there will be a clear shift in molecular weight of crosslinked versus non-crosslinked proteins (50).

Determining whether KDM4A affects the stability of the pBAF complex can be carried out by simply knocking down KDM4A and monitoring the expression level of the pBAF subunits through SDS-PAGE and WB analysis. In addition, since KDM4A influences transcription, it would be optimal to also analyze the mRNA levels of the subunits of the pBAF complex. In this way we will be interpreting whether KDM4A solely affects the stability of the pBAF complex. In addition, KDM4A was found to direct AP1 transcription factor to its gene targets (9). Co-localization of the pBAF complex with KDM4A can be determined through chromatin IP (ChIP) assay. In this case, a KDM4A ChIP and ARID2 ChIP can determine if KDM4A and the pBAF complex localize to similar chromatin regions. ChIP assay is an ideal experiment that can be used in this context since it will pinpoint the proteins linked to a certain chromatin region (75). In this case we are interested in the regions that overlap between KDM4A and ARID2. Furthermore, since ARID2 plays an important role in directing the pBAF complex to different genes, then we can assume that the shared regions are also frequented by the pBAF complex (53). In addition, to further analyze the role of KDM4A on the stability of the pBAF complex, we can perform ARID2 ChIP assay in the context of KDM4A knockdown.

4.7.3 Validation of role of KDM4A in stable expression of COX-2

To determine the involvement of KDM4A in the stable expression of COX-2, we can knockdown KDM4A and/or ELVAL1 and monitor the protein expression of COX-2 through WB analysis. According to our results, KDM4A-ELVAL1 protein interaction seems to be dependent on KDM4A's TT domain and catalytic activity. A FLAG IP with KDM4A, KDM4A^{H188A}, and KDM4A-ΔTT would confirm these results, where FLAG-GFP would be used as a control.

4.7.4 Validation of role of KDM4A in protein stabilization

The stability of proteins can be measured by cycloheximide chase analysis, which measures protein degradation using cycloheximide, a fungicide (63). Cycloheximide blocks translation by preventing the binding of the eukaryotic elongation factor to the ribosome (63,105). Consequently, proteins are being degraded over time. This will enable the monitoring of

proteins that were synthesized before the addition of cycloheximide. In other words, since synthesis of new proteins is inhibited, protein degradation can be more accurately observed as there is no new input to the overall pool of proteins. Furthermore, using this experiment, we could associate KDM4A to the stability of a protein by measuring the levels of the protein of interest in the presence or absence of KDM4A. This can be monitored with WB analysis or quantitative MS (63).

5. Concluding Remarks

In this study we have presented and analyzed the results of potential KDM4A interactors in the context of cervical cancer. We have pinpointed the dependability of some of these proteins on the catalytic activity and/or the TT domain of KDM4A. We proposed novel functions of KDM4A and have concluded that KDM4A could be interacting with the pBAF chromatin remodeling complex, ELAVL1, a protein responsible for mRNA stability (59), and organic anion transporters. All these interactions could be contributing factors of carcinogenesis (54,55,59,60,62,72). Our results also showed that the interaction of KDM4A with the DDR protein seems to be dependent on the TT domain. Taking all this into account, these analyses open a wide range of potential branches of KDM4A functionality that should be further studied in the context of cancer and therapeutics.

References

1. Dang C., Gilewski TA, Surbone A, Norton L. Cell Proliferation [Internet]. In: Kufe DW, Pollock RE, Weichselbaum RR, et al., editors. Holland-Frei Cancer Medicine. 6th edition. Hamilton (ON): BC Decker; 2003. Available from: https://www.ncbi.nlm.nih.gov/books/NBK12640/

2. Barnum KJ, O'Connell MJ. Cell cycle regulation by checkpoints. Methods in molecular biology (Clifton, NJ). 2014;1170:29-40.

3. Stewart ZA, Westfall MD, Pietenpol JA. Cell-cycle dysregulation and anticancer therapy. Trends in Pharmacological Sciences. 2003;24(3):139-45.

4. Feitelson MA, Arzumanyan A, Kulathinal RJ, Blain SW, Holcombe RF, Mahajna J, et al. Sustained proliferation in cancer: Mechanisms and novel therapeutic targets. Seminars in cancer biology. 2015;35 Suppl(Suppl):S25-S54.

5. Cheng Y, He C, Wang M, Ma X, Mo F, Yang S, et al. Targeting epigenetic regulators for cancer therapy: mechanisms and advances in clinical trials. Signal Transduct Target Ther. 2019;4:62.

6. Chen QW, Zhu XY, Li YY, Meng ZQ. Epigenetic regulation and cancer (review). Oncol Rep. 2014;31(2):523-32.

7. Berry WL, Janknecht R. KDM4/JMJD2 histone demethylases: epigenetic regulators in cancer cells. Cancer Res. 2013;73(10):2936-42.

8. Guerra-Calderas L, González-Barrios R, Herrera LA, Cantú de León D, Soto-Reyes E. The role of the histone demethylase KDM4A in cancer. Cancer Genetics. 2015;208(5):215-24.

9. Labbe RM, Holowatyj A, Yang ZQ. Histone lysine demethylase (KDM) subfamily 4: structures, functions and therapeutic potential. Am J Transl Res. 2013;6(1):1-15.

10. Sanchez R, Zhou MM. The PHD finger: a versatile epigenome reader. Trends Biochem Sci. 2011;36(7):364-72.

11. Kim SM, Kim JS. A Review of Mechanisms of Implantation. Dev Reprod. 2017;21(4):351-9.

12. Sankar A, Kooistra SM, Gonzalez JM, Ohlsson C, Poutanen M, Helin K. Maternal expression of the histone demethylase Kdm4a is crucial for pre-implantation development. Development. 2017;144(18):3264.

13. Wu L, Wary Kishore K, Revskoy S, Gao X, Tsang K, Komarova Yulia A, et al. Histone Demethylases KDM4A and KDM4C Regulate Differentiation of Embryonic Stem Cells to Endothelial Cells. Stem Cell Reports. 2015;5(1):10-21.

14. Alabert C, Groth A. Chromatin replication and epigenome maintenance. Nature Reviews Molecular Cell Biology. 2012;13(3):153-67.

15. Black JC, Allen A, Van Rechem C, Forbes E, Longworth M, Tschöp K, et al. Conserved Antagonism between JMJD2A/KDM4A and HP1γ during Cell Cycle Progression. Molecular Cell. 2010;40(5):736-48.

16. Jackson SP, Bartek J. The DNA-damage response in human biology and disease. Nature. 2009 Oct 22;461(7267):1071-8. PubMed PMID: 19847258. PMCID: PMC2906700. Epub 2009 Oct 23. eng.

17. Giglia-Mari G, Zotter A, Vermeulen W. DNA damage response. Cold Spring Harb Perspect Biol. 2011 Jan 1;3(1):a000745. PubMed PMID: 20980439. PMCID: PMC3003462. Epub 2010/10/29. eng.

18. Mallette FA, Mattiroli F, Cui G, Young LC, Hendzel MJ, Mer G, et al. RNF8- and RNF168-dependent degradation of KDM4A/JMJD2A triggers 53BP1 recruitment to DNA damage sites. The EMBO journal. 2012;31(8):1865-78.

19. Mirza-Aghazadeh-Attari M, Mohammadzadeh A, Yousefi B, Mihanfar A, Karimian A, Majidinia M. 53BP1: A key player of DNA damage response with critical functions in cancer. DNA Repair (Amst). 2019;73:110-9.

20. van Deursen JM. The role of senescent cells in ageing. Nature. 2014;509(7501):439-46.

21. Liu X-l, Ding J, Meng L-h. Oncogene-induced senescence: a double edged sword in cancer. Acta Pharmacologica Sinica. 2018;39(10):1553-8.

22. Iannello A, Thompson TW, Ardolino M, Lowe SW, Raulet DH. p53-dependent chemokine production by senescent tumor cells supports NKG2D-dependent tumor elimination by natural killer cells. Journal of Experimental Medicine. 2013;210(10):2057-69.

23. Pazolli E, Alspach E, Milczarek A, Prior J, Piwnica-Worms D, Stewart SA. Chromatin Remodeling Underlies the Senescence-Associated Secretory Phenotype of Tumor Stromal Fibroblasts That Supports Cancer Progression. Cancer Research. 2012;72(9):2251-61.

24. Fernández E, Mallette FA. The Rise of FXR1: Escaping Cellular Senescence in Head and Neck Squamous Cell Carcinoma. PLoS genetics. 2016;12(11):e1006344-e.

25. Guerra-Calderas L, González-Barrios R, Patiño CC, Alcaraz N, Salgado-Albarrán M, de León DC, et al. CTCF-KDM4A complex correlates with histone modifications that negatively regulate CHD5 gene expression in cancer cell lines. Oncotarget. 2018;9(24):17028-42.

26. Mallette Frédérick A, Richard S. JMJD2A Promotes Cellular Transformation by Blocking Cellular Senescence through Transcriptional Repression of the Tumor Suppressor CHD5. Cell Reports. 2012;2(5):1233-43.

27. Black JC, Manning AL, Van Rechem C, Kim J, Ladd B, Cho J, et al. KDM4A lysine demethylase induces site-specific copy gain and rereplication of regions amplified in tumors. Cell. 2013;154(3):541-55.

28. Carbonneau M, L MG, Lalonde ME, Germain MA, Motorina A, Guiot MC, et al. The oncometabolite 2-hydroxyglutarate activates the mTOR signalling pathway. Nat Commun. 2016;7:12700.

29. Li M, Cheng J, Ma Y, Guo H, Shu H, Huang H, et al. The histone demethylase JMJD2A promotes glioma cell growth via targeting Akt-mTOR signaling. Cancer Cell Int. 2020;20:101.

30. Porta C, Paglino C, Mosca A. Targeting PI3K/Akt/mTOR Signaling in Cancer. Front Oncol. 2014;4:64.

31. Cui SZ, Lei ZY, Guan TP, Fan LL, Li YQ, Geng XY, et al. Targeting USP1-dependent KDM4A protein stability as a potential prostate cancer therapy. Cancer Sci. 2020.

32. Tan MK, Lim HJ, Harper JW. SCF(FBXO22) regulates histone H3 lysine 9 and 36 methylation levels by targeting histone demethylase KDM4A for ubiquitin-mediated proteasomal degradation. Mol Cell Biol. 2011;31(18):3687-99.

33. Agger K, Miyagi S, Pedersen MT, Kooistra SM, Johansen JV, Helin K. Jmjd2/Kdm4 demethylases are required for expression of Il3ra and survival of acute myeloid leukemia cells. Genes Dev. 2016;30(11):1278-88.

34. Mar BG, Chu SH, Kahn JD, Krivtsov AV, Koche R, Castellano CA, et al. SETD2 alterations impair DNA damage recognition and lead to resistance to chemotherapy in leukemia. Blood. 2017;130(24):2631-41.

35. Li Y, Wang Yn, Xie Z, Hu H. JMJD2A facilitates growth and inhibits apoptosis of cervical cancer cells by downregulating tumor suppressor miR-491-5p. Molecular medicine reports. 2019;19(4):2489-96.

36. Lee DH, Kim GW, Jeon YH, Yoo J, Lee SW, Kwon SH. Advances in histone demethylase KDM4 as cancer therapeutic targets. The FASEB Journal. 2020;34(3):3461-84.

37. Soto D, Song C, McLaughlin-Drubin ME. Epigenetic Alterations in Human Papillomavirus-Associated Cancers. Viruses. 2017;9(9).

38. Dickinson JA, Stankiewicz A, Popadiuk C, Pogany L, Onysko J, Miller AB. Reduced cervical cancer incidence and mortality in Canada: national data from 1932 to 2006. BMC public health. 2012;12:992-.

39. Subramaniam A, Fauci JM, Schneider KE, Whitworth JM, Erickson BK, Kim K, et al. Invasive cervical cancer and screening: what are the rates of unscreened and underscreened women in the modern era? J Low Genit Tract Dis. 2011;15(2):110-3.

40. Kim DI, Birendra KC, Zhu W, Motamedchaboki K, Doye V, Roux KJ. Probing nuclear pore complex architecture with proximity-dependent biotinylation. Proc Natl Acad Sci U S A. 2014;111(24):E2453-61.

41. Kim DI, Jensen SC, Noble KA, Kc B, Roux KH, Motamedchaboki K, et al. An improved smaller biotin ligase for BioID proximity labeling. Mol Biol Cell. 2016;27(8):1188-96.

42. Che Y, Khavari PA. Research Techniques Made Simple: Emerging Methods to Elucidate Protein Interactions through Spatial Proximity. J Invest Dermatol. 2017;137(12):e197-e203.

43. Samavarchi-Tehrani P, Abdouni H, Samson R, Gingras A-C. A Versatile Lentiviral Delivery Toolkit for Proximity-dependent Biotinylation in Diverse Cell Types. Molecular & Cellular Proteomics. 2018;17(11):2256.

44. Wang LY, Hung CL, Chen YR, Yang JC, Wang J, Campbell M, et al. KDM4A Coactivates E2F1 to Regulate the PDK-Dependent Metabolic Switch between Mitochondrial Oxidation and Glycolysis. Cell Rep. 2016;16(11):3016-27.

45. Kim TD, Jin F, Shin S, Oh S, Lightfoot SA, Grande JP, et al. Histone demethylase JMJD2A drives prostate tumorigenesis through transcription factor ETV1. J Clin Invest. 2016;126(2):706-20.

46. Wang J, Wang H, Wang LY, Cai D, Duan Z, Zhang Y, et al. Silencing the epigenetic silencer KDM4A for TRAIL and DR5 simultaneous induction and antitumor therapy. Cell Death Differ. 2016;23(11):1886-96.

47. Gray SG, Iglesias AH, Lizcano F, Villanueva R, Camelo S, Jingu H, et al. Functional characterization of JMJD2A, a histone deacetylase- and retinoblastoma-binding protein. J Biol Chem. 2005;280(31):28507-18.

48. Kim T-D, Shin S, Berry WL, Oh S, Janknecht R. The JMJD2A demethylase regulates apoptosis and proliferation in colon cancer cells. Journal of Cellular Biochemistry. 2012;113(4):1368-76.

49. Liu Y, West SC. Distinct functions of BRCA1 and BRCA2 in double-strand break repair. Breast Cancer Res. 2002;4(1):9-13.

50. Detection of protein-protein interactions using the GST fusion protein pull-down technique. Nature Methods. 2004;1(3):275-6.

51. Mintseris J, Gygi SP. High-density chemical cross-linking for modeling protein interactions. Proceedings of the National Academy of Sciences. 2020;117(1):93-102.

52. Hodges C, Kirkland JG, Crabtree GR. The Many Roles of BAF (mSWI/SNF) and PBAF Complexes in Cancer. Cold Spring Harbor perspectives in medicine. 2016;6(8):a026930.

53. Yan Z, Cui K, Murray DM, Ling C, Xue Y, Gerstein A, et al. PBAF chromatin-remodeling complex requires a novel specificity subunit, BAF200, to regulate expression of selective interferon-responsive genes. Genes & development. 2005;19(14):1662-7. Epub 2005/06/28.

54. Hakimi AA, Attalla K, DiNatale RG, Ostrovnaya I, Flynn J, Blum KA, et al. A pan-cancer analysis of PBAF complex mutations and their association with immunotherapy response. Nature Communications. 2020;11(1):4168.

55. Pan D, Kobayashi A, Jiang P, Ferrari de Andrade L, Tay RE, Luoma AM, et al. A major chromatin regulator determines resistance of tumor cells to T cell-mediated killing. Science (New York, NY). 2018;359(6377):770-5. Epub 2018/01/04.

56. Yu P, Wu D, You Y, Sun J, Lu L, Tan J, et al. miR-208-3p promotes hepatocellular carcinoma cell proliferation and invasion through regulating ARID2 expression. Experimental Cell Research. 2015;336(2):232-41.

57. Zhang L, Wang W, Li X, He S, Yao J, Wang X, et al. MicroRNA-155 promotes tumor growth of human hepatocellular carcinoma by targeting ARID2. Int J Oncol. 2016;48(6):2425-34.

58. Zhao H, Wang J, Han Y, Huang Z, Ying J, Bi X, et al. ARID2: a new tumor suppressor gene in hepatocellular carcinoma. Oncotarget. 2011;2(11):886-91.

59. Lim S-J, Kim HJ, Kim JY, Park K, Lee C-M. Expression of HuR Is Associated With Increased Cyclooxygenase-2 Expression in Uterine Cervical Carcinoma. International Journal of Gynecological Pathology. 2007;26(3).

60. Wang J, Guo Y, Chu H, Guan Y, Bi J, Wang B. Multiple functions of the RNA-binding protein HuR in cancer progression, treatment responses and prognosis. International journal of molecular sciences. 2013;14(5):10015-41.

61. Xue F, Li QR, Xu YH, Zhou HB. MicroRNA-139-3p Inhibits The Growth And Metastasis Of Ovarian Cancer By Inhibiting ELAVL1. OncoTargets and therapy. 2019;12:8935-45.

62. Edemir B. Identification of Prognostic Organic Cation and Anion Transporters in Different Cancer Entities by In Silico Analysis. International journal of molecular sciences. 2020;21(12):4491.

63. Buchanan BW, Lloyd ME, Engle SM, Rubenstein EM. Cycloheximide Chase Analysis of Protein Degradation in Saccharomyces cerevisiae. Journal of visualized experiments: JoVE. 2016(110):53975.

64. Majumder M, House R, Palanisamy N, Qie S, Day TA, Neskey D, et al. RNA-Binding Protein FXR1 Regulates p21 and TERC RNA to Bypass p53-Mediated Cellular Senescence in OSCC. PLoS Genet. 2016;12(9):e1006306.

65. Saleh T, Tyutynuk-Massey L, Cudjoe EK, Jr., Idowu MO, Landry JW, Gewirtz DA. Non-Cell Autonomous Effects of the Senescence-Associated Secretory Phenotype in Cancer Therapy. Frontiers in oncology. 2018;8:164.

66. Van Rechem C, Black JC, Boukhali M, Aryee MJ, Gräslund S, Haas W, et al. Lysine demethylase KDM4A associates with translation machinery and regulates protein synthesis. Cancer discovery. 2015;5(3):255-63. Epub 2015/01/06.

67. Escors D, Breckpot K. Lentiviral vectors in gene therapy: their current status and future potential. Archivum immunologiae et therapiae experimentalis. 2010;58(2):107-19. Epub 2010/02/09.

68. Kallunki T, Barisic M, Jäättelä M, Liu B. How to Choose the Right Inducible Gene Expression System for Mammalian Studies? Cells. 2019;8(8):796.

69. Johmura Y, Sun J, Kitagawa K, Nakanishi K, Kuno T, Naiki-Ito A, et al. SCFFbxo22-KDM4A targets methylated p53 for degradation and regulates senescence. Nature Communications. 2016;7(1):10574.

70. Marouco D, Garabadgiu AV, Melino G, Barlev NA. Lysine-specific modifications of p53: a matter of life and death? Oncotarget. 2013;4(10):1556-71.

71. Agalioti T, Lomvardas S, Parekh B, Yie J, Maniatis T, Thanos D. Ordered recruitment of chromatin modifying and general transcription factors to the IFN-beta promoter. Cell. 2000;103(4):667-78. Epub 2000/12/07.

72. Choi S-H, Kim M-Y, Yoon Y-S, Koh D-I, Kim M-K, Cho S-Y, et al. Hypoxia-induced RelA/p65 derepresses SLC16A3 (MCT4) by downregulating ZBTB7A. Biochimica et Biophysica Acta (BBA) - Gene Regulatory Mechanisms. 2019;1862(8):771-85.

73. Muz B, de la Puente P, Azab F, Azab AK. The role of hypoxia in cancer progression, angiogenesis, metastasis, and resistance to therapy. Hypoxia (Auckland, NZ). 2015;3:83-92.

74. Dobrynin G, McAllister TE, Leszczynska KB, Ramachandran S, Krieg AJ, Kawamura A, et al. KDM4A regulates HIF-1 levels through H3K9me3. Scientific Reports. 2017;7(1):11094.

75. Sasaki S, Futagi Y, Ideno M, Kobayashi M, Narumi K, Furugen A, et al. Effect of diclofenac on SLC16A3/MCT4 by the Caco-2 cell line. Drug Metabolism and Pharmacokinetics. 2016;31(3):218-23.

76. Brú A, Albertos S, Luis Subiza J, García-Asenjo JL, Brú I. The universal dynamics of tumor growth. Biophysical Journal. 2003;85(5):2948-61.

77. Das-Bradoo S, Bielinsky A. DNA Replication and Checkpoint Control in S Phase. Nature Education 2010;3(9):50.

78. Cooper GM. Regulators of Cell Cycle Progression. The Cell: A Molecular Approach. 2nd edition. Sunderland (MA): Sinauer Associates; 2000.

79. Otto T, Sicinski P. Cell cycle proteins as promising targets in cancer therapy. Nature Reviews Cancer. 2017;17(2):93-115.

80. Stamatakos M, Palla V, Karaiskos I, Xiromeritis K, Alexiou I, Pateras I, Kontzoglou K. Cell cyclins: triggering elements of cancer or not? World Journal of Surgical Oncology. 2010;8:111.

81. Cooper GM. The Development and Causes of Cancer. The Cell: A Molecular Approach. 2nd edition. Sunderland (MA): Sinauer Associates; 2000.

82. Cheung HH, Lee TL, Rennert OM, Chan WY. DNA methylation of cancer genome. Birth Defects Research Part C: Embryo Today. 2009;87(4):335-50.

83. Asghar U, Witkiewicz AK, Turner NC, Knudsen ES. The history and future of targeting cyclin-dependent kinases in cancer therapy. Nat Reviews Drug Discovery. 2015;14(2):130-46.

84. Jia P, Zhao Z. Impacts of somatic mutations on gene expression: an association perspective. Briefing Bioinformatics. 2017;18(3):413-425.

85. Gerstung M, Pellagatti A, Malcovati L, Giagounidis A, Porta MG, Jädersten M, et al. Combining gene mutation with gene expression data improves outcome prediction in myelodysplastic syndromes. Nature Communications. 2015;6:5901.

86. Lowe BR, Maxham LA, Hamey JJ, Wilkins MR, Partridge JF. Histone H3 Mutations: An Updated View of Their Role in Chromatin Deregulation and Cancer. Cancers (Basel). 2019;11(5):660.

87. Salifou K, Ray S, Verrier L, Aguirrebengoa M, Trouche D, Panov KI, Vandromme M. The histone demethylase JMJD2A/KDM4A links ribosomal RNA transcription to nutrients and growth factors availability. Nature Communications 2016;7:10174.

88. Ibrahim SAE, Abudu A, Johnson E, Aftab N, Conrad S, Fluck M. The role of AP-1 in self-sufficient proliferation and migration of cancer cells and its potential impact on an autocrine/paracrine loop. Oncotarget. 2018;9(76):34259-34278.

89. Kim SM, Kim JS. A Review of Mechanisms of Implantation. Development & Reproduction. 2017 Dec;21(4):351-359. doi: 10.12717/DR.2017.21.4.351. Epub 2017 Dec 31.

90. Sankar A, Lerdrup M, Manaf A, Johansen JV, Gonzalez JM, Borup R, et al. KDM4A regulates the maternal-to-zygotic transition by protecting broad H3K4me3 domains from H3K9me3 invasion in oocytes. Nature Cell Biology. 2020;22(4):380-8.

91. Tang Y, Chen Z-y, Hong Y-z, Wu Q, Lin H-q, Chen CD, et al. Expression profiles of histone lysine demethylases during cardiomyocyte differentiation of mouse embryonic stem cells. Acta Pharmacologica Sinica. 2014;35(7):899-906.

92. Neault M, Mallette FA, Richard S. miR-137 Modulates a Tumor Suppressor Network-Inducing Senescence in Pancreatic Cancer Cells. Cell Reports. 2016;14(8):1966-1978.

93. Advani SH. Targeting mTOR pathway: A new concept in cancer therapy. Indian Journal of Medical and Paediatric Oncology. 2010;31(4):132-6.

94. Catena V & Fanciulli M. Deptor: not only a mTOR inhibitor. Journal of Experimental & Clinical Cancer Research. 2017;36(1):12.

95. Geybels MS, Fang M, Wright JL, Qu X, Bibikova M, Klotzle B, et al. PTEN loss is associated with prostate cancer recurrence and alterations in tumor DNA methylation profiles. Oncotarget. 2017;8(48):84338-84348.

96. Lonergan PE & Tindall DJ. Androgen receptor signaling in prostate cancer development and progression. J Carcinog. 2011;10:20. Epub 2011 Aug 23.

97. Xiao CY, Fu BB, Li ZY, Mushtaq G, Kamal MA, Li JH, Tang GC, Xiao SS. Observations on the expression of human papillomavirus major capsid protein in HeLa cells. Cancer Cell International. 2015;15:53.

98. Lucey BP, Nelson-Rees WA, Hutchins GM. Henrietta Lacks, HeLa Cells, and Cell Culture Contamination. Archives of Pathology & Laboratory Medicine. 2009;133(9):1463-7.

99. Denoyelle C, Lambert B, Meryet-Figuière M, Vigneron N, Brotin E, Lecerf C, et al. miR-491-5p-induced apoptosis in ovarian carcinoma depends on the direct inhibition of both BCL-XL and EGFR leading to BIM activation. Cell Death Disease. 2014;5: e1445.

100. Morrison AJ. Chromatin-remodeling links metabolic signaling to gene expression. Molecular Metabolism. 2020 Aug;38:100973.

101. Xue Y, Canman JC, Lee CS, Nie Z, Yang D, Moreno GT, Young MK, Salmon ED, Wang W. The human SWI/SNF-B chromatin-remodeling complex is related to yeast rsc and localizes at kinetochores of mitotic chromosomes. PNAS. 2000 Nov 21;97(24):13015-20.

102. Nie Z, Xue Y, Yang D, Zhou S, Deroo BJ, Archer TK, and Wang W. A specificity and targeting subunit of a human SWI/SNF family-related chromatin-remodeling complex. Molecular and Cellular Biology. 2000;20: 8879–8888.

103. García-Cárdenas JM, Guerrero S, López-Cortés A, Armendáriz-Castillo I, Guevara-Ramírez P, Pérez-Villa A, Yumiceba V, et al. Post-transcriptional Regulation of Colorectal Cancer: A Focus on RNA-Binding Proteins. Frontiers in Molecular Bioscience. 2019;6:65.

104. Yan S, Wang Y, Chen M, Li G, Fan J. Deregulated SLC2A1 Promotes Tumor Cell Proliferation and Metastasis in Gastric Cancer. International Journal of Molecular Sciences. 2015;16(7):16144-57.

105. Schneider-Poetsch T, Ju J, Eyler DE, Dang Y, Bhat S, Merrick WC, Green R, Shen B, Liu JO. Inhibition of eukaryotic translation elongation by cycloheximide and lactimidomycin. Nature Chemical Biology. 2010;6(3):209-21.